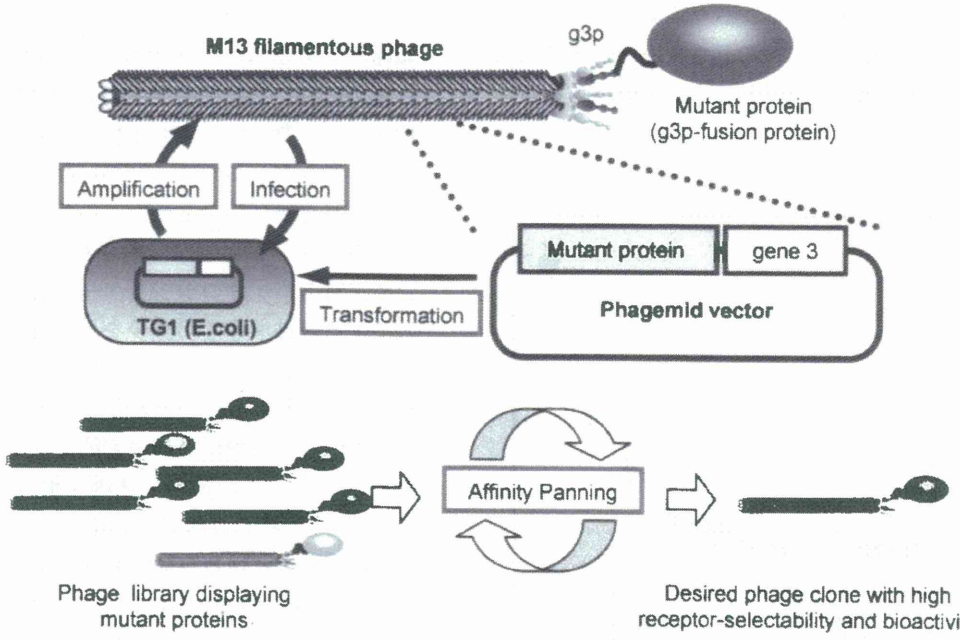

Fig. 1. Creation of Functional Mutant Proteins Using Phage Display

Phage display system has the following main characteristics: 1) proteins can be displayed on the outer shell of the phage where they can interact with their target molecules, such as a receptor or antigen. These protein-displaying phage particles are produced by the integration of a foreign gene into the 5'-terminus of the gene that encodes the outer shell of the phage (*i.e.*, g3p) in phagemid vector or phage genome; 2) the genotype of this phage (the foreign gene inside the phage clone), corresponds with the phenotype (the protein displayed on the phage's surface); 3) phage particles or "libraries", can readily be made, which consist of billions of varieties of protein; 4) a selected phage from the library can be readily amplified by infection of a host bacterial cell. It is therefore possible to screen for, and then isolate, high-affinity binders to target molecules from the phage library.

を駆使し，活性発現や三量体形成に重要な K11 や K65, K90 などを含む全 6 個のリジン残基を一挙に他のアミノ酸へ置換しても，wtTNF と同等さらには 10 倍以上もの生物活性やレセプター親和性を有する機能性リジン欠損 TNF 変異体を創出することに初めて成功している（Table 1）.[20] そこで本テクノロジーを駆使することで，TNF のレセプターとの結合領域に位置する計 6 ヵ所のアミノ酸残基を網羅的に他のアミノ酸に置換した構造変異 TNF 発現ファージライブラリを作製し，スクリーニングした結果，「TNFR2 とは結合せず，TNFR1 に対してのみ野生型 TNF と同等の結合親和性を示す TNFR1 指向性アンタゴニスト（TNF-T2）」が初めて創出できた（Fig. 2）.[21] これまで，生理活性タンパク質の構造変異体が野生型タンパク質により発現する生物活性に対してアンタゴニスト活性を示すという概念すらなく，この「タンパク性アンタゴニスト」とも言うべき TNFR1 指向性アンタゴニストの創出は，独自に構築した基盤テクノロジーを応用することで初めてなし得たものである．またレセプター指向性を有した TNF-T2 の創出基盤は，生物学的改変により特定のレセプターへのターゲティング能をタンパク質に付与できる点で，分子レベルの DDS であり，いわばタンパク医薬による疾病治療の最適化を目指した「生物学的 DDS」と位置づけられる．

Table 1. Amino Acid Sequences and *in vitro* Bioactivity of Lysine-deficient Mutant TNF (K90R)

	Residue Position						EC_{50}[1] (ng/ml)
	11	65	90	98	112	128	
wtTNF	K	K	K	K	K	K	1.28
K90R	A	S	R	A	L	T	0.12

[1] The bioactivities of wild-type TNF (wtTNF) and K90R were measured by cytotoxic assay using HEp-2 cells in the presence of cycloheximide (50 μg/ml). Experimental data were analyzed by a logistic regression model to calculate the mean effective concentration (EC50).

4. 高分子化学的 DDS による部位特異的バイオコンジュゲーション

関節リウマチなどの慢性炎症性疾患を対象とした検討においては，往々にして，血中濃度の維持を目的とした薬物の長期的な投与が必要であるが，

TNF-T2 も例外でない．タンパク性薬物の最大の問題点は，その生体内安定性の低さであると考えられる．そのため，慢性の疾患に対し TNF-T2 を用いる場合，この問題を克服し，長期投与にも耐え得る戦略が必要となる．主として 1980 年代以降，DDS を視野においた医薬品開発の分野において，生理活性タンパク質の生体内安定性を改善するために，ポリエチレングリコール（PEG）などの水溶性高分子をタンパク質に結合させた，いわゆる高分子バイオコンジュゲーションが考案されてきた．[22-24] このタンパク質のバイオコンジュゲーションは，分子量増大による腎排泄速度の減少をもたらすだけでなく，バイオコンジュゲーションに用いた修飾高分子によりタンパク質の分子表面が覆われるために，プロテアーゼからの攻撃が立体障害的にブロックされ，結果としてタンパク質の生体内半減期が延長される (Fig. 3)．同様の立体障害効果によって，免疫応答においても抗原性及び免疫原性が低下し，体内クリアランスの減少に直結する．以上に述べた総合的な体内安定化効果により，最終的にタンパク質の生体への投与量・回数を削減することが可能となる．このバイオコンジュゲーションは，数ある DDS の中でもタンパク質の医薬品化に向けた最適 DDS と位置づけられてきたが，依然としてその成功例は限られている．この最大の原因は，タンパク質の活性中

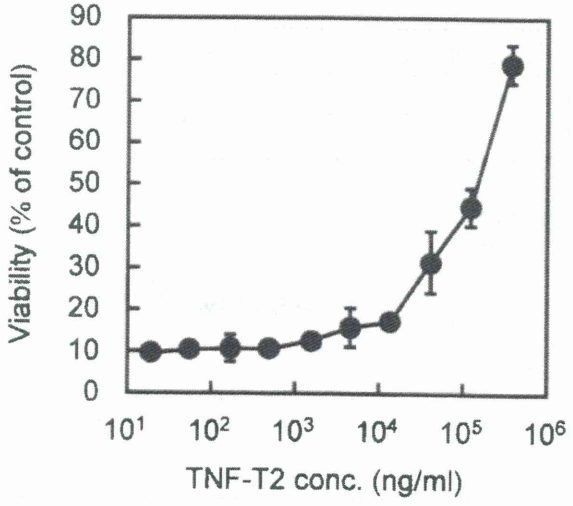

Fig. 2. Antagonistic Activities of the R1antTNF

Serial dilutions of TNF-T2 were mixed with human wtTNF (20 ng/ml) and then applied to HEp-2 cells. After 18 h, the inhibitory effects of TNF-T2 on the cytotoxicity of wtTNF were assessed by using the methylene blue assay. The absorbance of cells without wtTNF was plotted as 100 percent viability. The data represent the mean±SD (n=3).

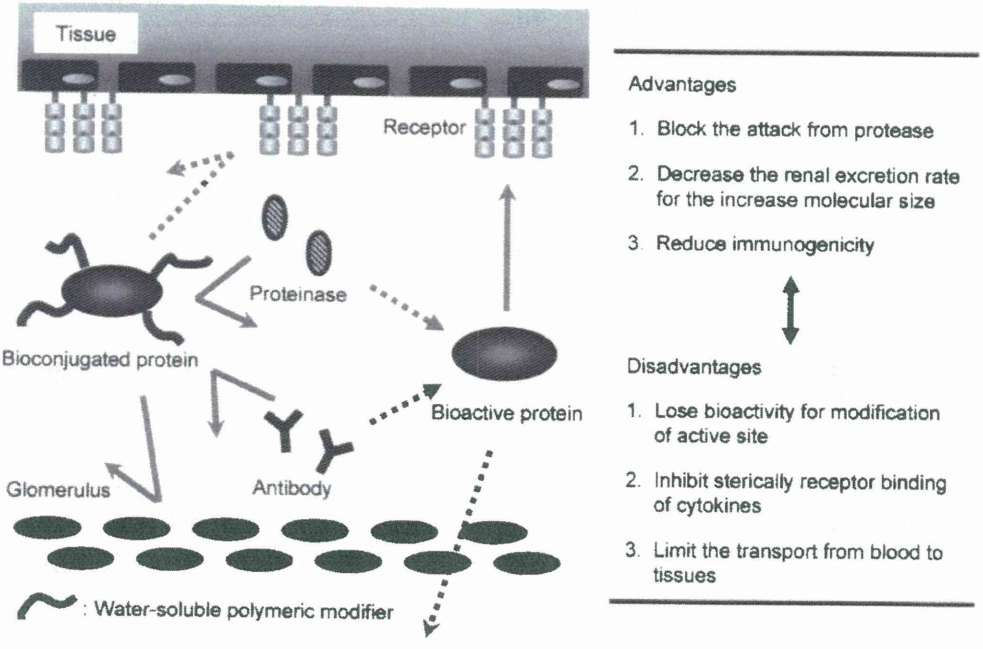

Fig. 3. Characteristics of Bioconjugation

Bioconjugated proteins with water-soluble polymeric modifiers increase their molecular size and steric hindrance, resulting in augmented plasma half-lives and stability.

心に存在するリジン残基へのランダムな水溶性高分子導入による致命的な比活性低下と，バイオコンジュゲート化タンパク質の分子的・機能的不均一性にある．事実，現在C型肝炎の特効薬として市販されているPEG化Interferon-α（PEGASYS）ですら，残存活性10–30%のヘテロ集団であることが報告されている．したがって，タンパク療法の最適化を目指したDDSを推進するためには，部位特異的に効率よく高分子導入でき，高い比活性を有するバイオコンジュゲート体を創製できる方法の確立が待望されている．

この点，筆者らが創出したTNFR1指向性アンタゴニストTNF-T2は，前述したリジン欠損TNF変異体をテンプレートに作製していること，*N*末端アミノ基は活性発現や立体構造形成に無関係であることから，そのアミノ基へのバイオコンジュゲーションを試みた場合，修飾高分子は*N*末端アミノ基にのみ導入されることになり，比活性低下を回避した上で，分子的均一性にも優れたバイオコンジュゲート体を作製可能である．これまでに，*N*末端部位特異的に修飾高分子PEGを導入したPEG化TNF-T2（PEG-T2）が，野生型TNF-T2と比較して，*in vitro*におけるアンタゴニスト活性を低下することなく，血中滞留性が飛躍的に増大していることを見い出している．なお，この革新的な部位特異的バイオコンジュゲーション（高分子化学的DDS）は，前述した生物学的DDSによって機能性リジン欠損タンパク質を創製することで初めて実現可能になるものであり，両テクノロジーの融合で，従来法の諸問題を一挙に克服することに成功したものである．そこで，PEG-T2の新規自己免疫疾患治療薬としての有効性を評価するため，関節リウマチの動物モデルにおける関節炎抑制効果の検討と，既存のTNF阻害薬で致命的問題となっている感染症リスクに及ぼす影響を評価したところ，既存の抗TNF薬とは決定的に異なり，宿主のウイルス感染防御能に全く影響することなく，安全に，関節炎抑制効果を発揮することが判明している（Fig. 4）．すなわち，TNF-T2は内因性のTNFのTNFR2を介した感染防御作用になんら影響しないため，既存の抗TNF阻害薬の致命的問題点であった感染症リスクを回避できることから，安全かつ有効な自己免疫疾患治療薬となり得ることが示された．現在，TNF-T2のさらなる有用性を評価すべく，他の自己免疫疾患モデルに対しての治療実験を進めるとともに，霊長類レベルで医薬品化（関節リウマチ及び多発性硬化症を対象）を目指した研究ステージに移行している．

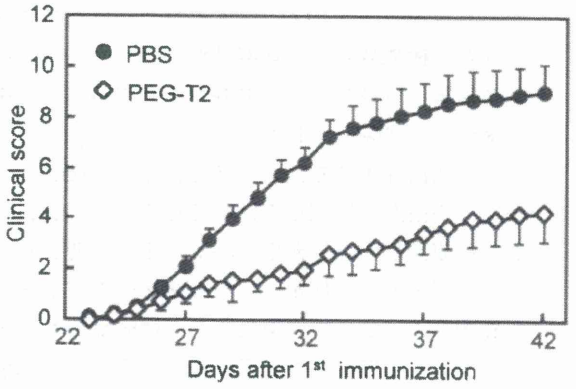

Fig. 4. Clinical Score of Collagen-induced Arthritis (CIA) Mice Treated with PEG-T2

The severity of arthritis in CIA mice ($n=10$) treated with PBS, PEG-T2 (1 μg twice a day) for three weeks from 23 day was assessed every day using an established macroscopic scoring system. Data of severity represent the mean±SEM.

5. おわりに

本稿では，タンパク質そのものに標的指向性を付与する“分子レベルの生物学的DDS”と，機能性人工タンパク質の体内動態制御を可能とする“生体レベルの高分子化学的DDS”の融合開発が，安全かつ有効な次世代型バイオ医薬品の創薬基盤となり得ることを示した．また，プロテオーム創薬は，プロテオミクス及び構造ゲノミクスの進展と，これらの知見を統括したバイオインフォマティクスが駆動力となり，近い将来，上記の「プロテオーム創薬システム」との融合により加速度的に推進されるものと期待される．すなわちこのようなプロテオーム創薬を指向したバイオインフォマティクスの進展は，タンパク質のアミノ酸配列と立体構造，機能との連関を理解可能とするため，近未来的にはタンパク質をコードした塩基配列やタンパク質のアミノ酸配列さえ判明すれば，その立体構造と機能が予測できることになる．これは逆に目的とする機能や立体構造を有した機能性タンパク質の新規デザインを可能とするだけでなく，タンパク質の立体構造やその機能を模倣した低分子化合物の合理的設計をも可能にするものと期待される．このようなバイオインフォマ

ティクスをシステムアップするためには，未知タンパク質の機能解明や立体構造解析に加え，種々のタンパク質について膨大な多様性を有する構造変異体を網羅的に作製し，レセプター・リガンド結合の様式，生物活性等をも含めた機能情報を集積し，立体構造との連関を追求しなければならない．この点筆者らが開発した分子進化戦略は，視点を変えればわずか1週間で1億種類以上もの多様性を有する構造変異体ライブラリを作製し，その機能情報をハイスループットに集積できる基盤技術と言える．本観点から現在，機能性人工TNFを含む様々な構造変異タンパク質の構造-活性相関情報の集積とともに構造情報を基にした低分子阻害剤のドラッグデザインへの研究展開を図ろうとしている．

謝辞　本研究は，㈱医薬基盤研究所創薬プロテオミクスプロジェクトプロジェクトリーダー・大阪大学薬学研究科毒性学分野教授　堤　康央先生，㈱医薬基盤研究所創薬プロテオミクスプロジェクトサブリーダー　角田慎一先生，同主任研究員　鎌田春彦先生をはじめとする多くの先生方のご指導のもと，㈱医薬基盤研究所創薬プロテオミクスプロジェクト（大阪大学大学院薬学研究科連携大学院医薬基盤科学分野），及び㈱林原生物化学研究所の皆さまとの共同成果であり，この場をお借りして，御礼を申し上げます．また種々ご指導，ご助言を賜りました大阪大学大学院薬学研究科薬剤学分野教授　中川晋作先生，同助教　向　洋平先生，大阪大学臨床医工学教育研究（MEI）センター講師　吉岡靖雄先生，大阪大学大学院薬学研究科毒性学分野助教　吉川友章先生，国立医薬品食品衛生研究所薬品部　柴田寛子先生，㈱医薬品・医療機器総合機構　杉田敏樹先生に深謝申し上げます．

REFERENCES

1) Hanash S., *Nature*, **422**, 226–232 (2003).
2) Gordon M. S., Nemunaitis J., Hoffman R., Paquette R. L., Rosenfeld C., Manfreda S., Isaacs R., Nimer S. D., *Blood*, **85**, 3066–3076 (1995).
3) Kreitman R. J., Wilson W. H., Bergeron K., Raggio M., Stetler-Stevenson M., FitzGerald D. J., Pastan I., *N. Eng. J. Med.*, **345**, 241–247 (2001).
4) Nagata S., *Nat. Med.*, **6**, 502–503 (2000).
5) Aderka D., Engelmann H., Maor Y., Brakebusch C., Wallach D., *J. Exp. Med.*, **175**, 323–329 (1992).
6) Feldmann M., Maini R. N., *Nat. Med.*, **9**, 1245–1250 (2003).
7) Muto Y., Nouri-Aria K. T., Meager A., Alexander G. J., Eddleston A. L., Williams R., *Lancet*, **2**, 72–74 (1988).
8) Breedveld F. C., Emery P., Keystone E., Patel K., Furst D. E., Kalden J. R., St Clair E. W., Weisman M., Smolen J., Lipsky P. E., Maini R. N., *Ann. Rheum. Dis.*, **63**, 149–155 (2004).
9) Genovese M. C., Bathon J. M., Martin R. W., Fleischmann R. M., Tesser J. R., Schiff M. H., Keystone E. C., Wasko M. C., Moreland L. W., Weaver A. L., Markenson J., Cannon G. W., Spencer-Green G., Finck B. K., *Arthritis Rheum.*, **46**, 1443–1450 (2002).
10) Gomez-Reino J. J., Carmona L., Valverde V. R., Mola E. M., Montero M. D., *Arthritis Rheum.*, **48**, 2122–2127 (2003).
11) Lubel J. S., Testro A. G., Angus P. W., *Intern. Med. J.*, **37**, 705–712 (2007).
12) Sicotte N. L., Voskuhl R. R., *Neurology*, **57**, 1885–1888 (2001).
13) Mori L., Iselin S., De Libero G., Lesslauer W., *J. Immunol.*, **157**, 3178–3182 (1996).
14) Kassiotis G., Kollias G., *J. Exp. Med.*, **193**, 427–434 (2001).
15) Liu J., Marino M. W., Wong G., Grail D., Dunn A., Bettadapura J., Slavin A. J., Old L., Bernard C. C., *Nat. Med.*, **4**, 78–83 (1998).
16) Engelmann H., Holtmann H., Brakebusch C., Avni Y. S., Sarov I., Nophar Y., Hadas E., Leitner O., Wallach D., *J. Biol. Chem.*, **265**, 14497–14504 (1990).
17) Adams G., Vessillier S., Dreja H., Chernajovsky Y., *Nat. Biotechnol.*, **21**, 1314–1320 (2003).
18) Sarkar C. A., Lowenhaupt K., Horan T., Boone T. C., Tidor B., Lauffenburger D. A., *Nat. Biotechnol.*, **20**, 908–913 (2002).
19) Zeytun A., Jeromin A., Scalettar B. A., Waldo G. S., Bradbury A. R., *Nat. Biotechnol.*, **21**, 1473–1479 (2003).
20) Yamamoto Y., Tsutsumi Y., Yoshioka Y., Nishibata T., Kobayashi K., Okamoto T.,

Mukai Y., Shimizu T., Nakagawa S., Nagata S., Mayumi T., *Nat. Biotechnol.*, **21**, 546–552 (2003).
21) Shibata H., Yoshioka Y., Ohkawa A., Minowa K., Mukai Y., Abe Y., Taniai M., Nomura T., Kayamuro H., Nabeshi H., Sugita T., Imai S., Nagano K., Yoshikawa T., Fujita T., Nakagawa S., Yamamoto A., Ohta T., Hayakawa T., Mayumi T., Vandenabeele P., Aggarwal B. B., Nakamura T., Yamagata Y., Tsunoda S., Kamada H., Tsutsumi Y., *J. Biol. Chem.*, **283**, 998–1007 (2008).
22) Harris J. M., Martin N. E., Modi M., *Clin. Pharmacokinet.*, **40**, 539–551 (2001).
23) Yamamoto Y., Tsutsumi Y., Mayumi T., *Curr. Drug Targets*, **3**, 123–130 (2002).
24) Youngster S., Wang Y. S., Grace M., Bausch J., Bordens R., Wyss D. F., *Curr. Pharm. Des.*, **8**, 2139–2157 (2002).

Biochemical and Biophysical Research Communications 388 (2009) 667–671

Contents lists available at ScienceDirect

Biochemical and Biophysical Research Communications

journal homepage: www.elsevier.com/locate/ybbrc

Novel protein engineering strategy for creating highly receptor-selective mutant TNFs

Tetsuya Nomura [a,b,1], Yasuhiro Abe [a,1], Haruhiko Kamada [a,c], Masaki Inoue [a], Tomoyuki Kawara [a,b], Shuhei Arita [a,b], Takeshi Furuya [a,b], Yasuo Yoshioka [b,c], Hiroko Shibata [a], Hiroyuki Kayamuro [a,b], Takuya Yamashita [a,b], Kazuya Nagano [a], Tomoaki Yoshikawa [a,b], Yohei Mukai [b], Shinsaku Nakagawa [b,c], Madoka Taniai [d], Tsunetaka Ohta [d], Shin-ichi Tsunoda [a,b,c,*], Yasuo Tsutsumi [a,b,c]

[a] National Institute of Biomedical Innovation (NiBio), 7-6-8 Saito-Asagi, Ibaraki, Osaka 567-0085, Japan
[b] Graduate School of Pharmaceutical Sciences, Osaka University, 1-6 Yamadaoka, Suita, Osaka 565-0871, Japan
[c] The Center for Advanced Medical Engineering and Informatics, Osaka University, 1-6 Yamadaoka, Suita, Osaka 565-0871, Japan
[d] Hayashibara Biochemical Laboratories Inc., 675-1 Fujisaki, Okayama 702-8006, Japan

ARTICLE INFO

Article history:
Received 4 August 2009
Available online 13 August 2009

Keywords:
Tumor necrosis factor (TNF)
Gene shuffling
Phage display technique
Protein engineering
TNF receptor-selective mutant

ABSTRACT

Tumor necrosis factor (TNF) plays important roles in host defense and in preventing tumor formation by acting via its receptors, TNFR1 and TNFR2, functions of which are less understood. To this end, we have been isolating TNF receptor-selective mutants using phage display technique. However, generation of a phage library with large repertoire (>10^8) is impeded by the limited transformation efficiency of *Escherichia coli*. Therefore, it is currently difficult to create a mutant library containing amino acid substitutions in more than seven residues. To overcome this problem, here we have used two different TNF mutant libraries, each containing random substitutions at six selected amino acid residues, and utilized a gene shuffling method to construct a randomized mutant library containing substitutions at 12 different amino acid residues of TNF. Consequently, using this library, we identified TNF mutants with greater receptor-selectivity and enhanced receptor-specific bioactivity than the existing mutants.

Introduction

Tumor necrosis factor-α (TNF) plays a critical role in host defense through regulation of cell survival, death, and inflammation by acting via one of its receptors, TNFR1 and TNFR2 [1]. Because excess or uncontrolled activity of TNF is often a cause for many immunological diseases and tumor development [2,3], biological drugs such as recombinant TNFs (for enhancement of TNF signaling) or anti-TNF monoclonal antibodies (Mab) and soluble TNF receptors (for neutralization of TNF signaling) have made significant impacts in the treatment of inflammatory diseases and in tumor therapy [4,5]. A number of published reports, however, suggested that neutralization of TNF resulted in increased risk of bacterial infection and several other side effects because of the blocking of signaling via both TNFR1 and TNFR2 [4,5]. Therefore, there is an urgent need to fully understand the biology of the TNF receptor mediated signaling pathway and to develop novel drugs for therapeutic use in TNF-related immunological diseases. For this purpose, TNF receptor-knockout mice were used to understand the relationship between the function of the TNF receptors and TNF-related diseases [8–10]. Recently, it was revealed that the two receptors worked together by crosstalk signaling, which suggested that the TNF-mediated signaling in the presence of both TNF receptors actually correlates with their physiological functions [1,6,7]. To elucidate the roles of TNFR1 and TNFR2, many researchers used an agonistic or an antagonistic TNF mutant that selectively binds to one of the receptors and initiates the biological activity of that specific receptor. These mutant TNFs might be a promising new class of TNF-related drugs without any side effect, and could as well serve as a tool for analyzing the receptor function. Development of these mutant TNFs has facilitated understanding of the molecular interaction between the TNF and its receptors, TNFR1 and TNFR2. In this context, it is noteworthy that several approaches have been undertaken to establish quantitative correlation between the receptor subtype specific-biological activity and the structural and kinetic binding parameters of a receptor-specific TNF mutant [8]. Mutational analysis of single amino acid residues revealed that amino acids at positions 15, 31–35, 84–87, 117, 119 and 143–148, which are clustered throughout in hotspots, greatly contributed to the biological activity of TNF [9,10].

* Corresponding author. Address: Laboratory of Pharmaceutical Proteomics, National Institute of Biomedical Innovation, 7-6-8 Saito-Asagi, Ibaraki, Osaka 567-0085, Japan. Fax: +81 72 641 9817.
E-mail address: tsunoda@nibio.go.jp (S.-i. Tsunoda).
[1] These authors contributed equally to the work.

0006-291X/$ - see front matter © 2009 Elsevier Inc. All rights reserved.
doi:10.1016/j.bbrc.2009.08.052

With a similar goal in mind, we previously constructed M13 bacteriophage libraries (Library I and Library II) displaying mutant TNFs randomized at amino acid positions 29, 31, 32, 145, 146 and 147 or at positions 84–89 of TNF, and succeeded in isolating agonistic- and antagonistic-mutant TNFs from these libraries [11,12]. Particularly, the TNFR1-selective antagonist mutTNF-T2 showed almost same therapeutic effect as the anti-TNF biologics in a hepatitis model [13].

Currently, generation of a phage-displayed library with large repertoire ($>10^8$) is impeded by the limited transformation efficiency of *Escherichia coli* (*E. coli*). As a result, it is difficult to construct a high quality mutant library ($20^6 = 6.4 \times 10^7$) that is randomized at more than seven different amino acid residues and includes almost all clones. To overcome this problem, here we have developed a novel protein engineering strategy (gene shuffling method) for creation of functional mutant proteins. To achieve our goal, we first constructed two types of phage libraries displaying mutant TNFs, in each of which six amino acids residues in the predicted receptor binding sites were replaced with other amino acid residues, and these phage display libraries were subsequently subjected to several rounds of panning against TNFR1 and TNFR2, respectively, using a surface plasmon resonance analyzer (BIAcore). After several rounds of panning, we obtained two libraries, each one containing enriched number of a TNF receptor-specific high affinity clones. Next, we utilized these enriched libraries to construct high quality TNF receptor-specific shuffling libraries using a gene shuffling method. Finally, panning of these shuffling libraries against TNFR1 and TNFR2, respectively, have allowed us to isolate TNF mutants with greater receptor-selectivity and enhanced receptor-specific bioactivity than the previously isolated TNFR1-selective mutant R1-5 and TNFR2-selective mutant R2-3 [12].

Materials and methods

Cell culture. HEp-2 cells (a human fibroblast cell line) were provided by the Cell Resource Center for Biomedical Research (Tohoku University, Sendai, Japan) and were maintained in RPMI 1640 medium (Sigma-Aldrich Japan, Tokyo, Japan) supplemented with 10% FBS and antibiotics cocktail (penicillin 10,000 units/ml, streptomycin 10 mg/ml, and amphotericin B 25 μg/ml; Nacalai tesque, Kyoto, Japan). hTNFR2/mFas-preadipocyte (mouse preadipocyte cell expressing a chimeric receptor, which consist of the extracellular and transmembrane domain of human TNFR2 and the intracellular domain of mouse Fas) cells were established previously in our laboratory [14] and were maintained in D-MEM (Wako Pure Chemical Industries, Osaka, Japan) supplemented with blasticidin S HCl (5 μg/ml Sigma-Aldrich Japan, Tokyo, Japan), 10% FBS, 1 mM sodium pyruvate, 5×10^{-5} M 2-mercaptoethanol, and antibiotic cocktail.

Selection of TNF receptor-selective mutants from the mutant TNF phage display library by panning. Human TNFR1 Fc chimera or human TNFR2 Fc chimera (R&D systems, Minneapolis, MN) was immobilized onto a CM3 sensor chip (GE Healthcare, Buckinghamshire, UK) as described previously [11,12]. The phage display library (1×10^{11} CFU/100 μl) was injected over the sensor chip at a flow rate of 3 μl/min on BIAcore. After binding, the chip was rinsed until the association phase was reached. Elution was carried out using 4 μl of 10 mM glycine–HCl. The eluted phage pool was neutralized with 1 M Tris–HCl (pH 6.9). Next, the phages in the eluted pool were amplified in the *E. coli* TG1. The panning, elution and amplification steps were repeated twice. Subsequently, single clones were isolated from the phage pool, and the DNA sequences of phagemids purified from the single clones were analyzed.

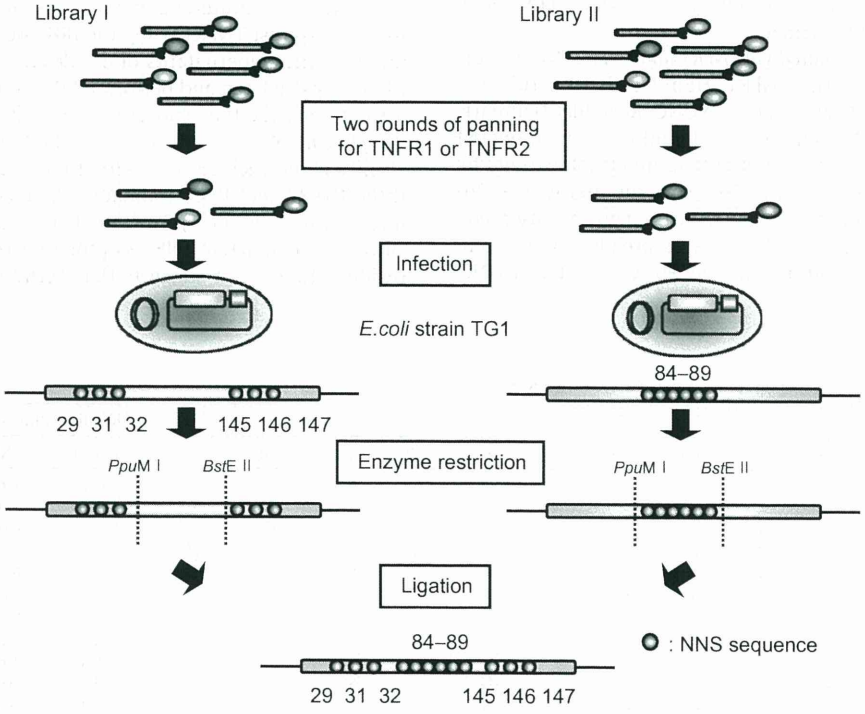

Fig. 1. Construction of the Gene Shuffling Library. Schematic description of the methods used to construct the Gene Shuffling Libraries A and B from two parent mutant TNF libraries, each one of which was created by replacing the codon of the amino acid residue at positions 29, 31, 32, 145, 146 and 147 (Library I) or at positions 84, 85, 86, 87, 88 and 89 (Library II) of TNF with the randomized codon NNS (where N and S represent G/A/T/C or G/C, respectively) to obtain all twenty amino acid substitutions at each position. NNS encodes all 20 different amino acids. Mutations were introduced by PCR using the lysine-deficient mutant TNF as the template as described in Materials and methods.

Construction of mutant TNF phage library (Gene Shuffling Library). The pCANTAB phagemid vector encoding a lysine-deficient mutant TNF which was created previously was used as a template for library construction [15]. First, two types of phage libraries, displaying mutant TNFs containing random substitutions of amino acid residues at positions 29, 31, 32, 145, 146 and 147 (Library I), and at positions 84, 85, 86, 87, 88 and 89 (Library II), were prepared using polymerase chain reaction (PCR) as described earlier [11,12]. Each library was then subjected to two rounds of panning against TNFR1 to concentrate TNFR1-specific high-affinity mutant TNFs. Next, we purified all plasmids from each concentrated libraries. These two pools of purified plasmids were digested with the restrict enzymes (*Ppu*MI, *Bst*EII), DNA inserts were purified and then ligated to a pY03′ phagemid vector to construct a randomized library (Shuffling Library A) that contained mutations at twelve different amino acid residues (see Fig. 1). We also prepared a second randomized library (Shuffling Library B) by following the same protocol and using TNFR2 for panning.

Competitive ELISA. Inhibition of wtTNF binding to the TNFR1 and TNFR2 by a TNFR1 or TNFR2-selective mutant was measured using ELISA as described previously [16]. The wtTNF-FLAG, a FLAG tag fusion protein of human TNF [16], was used as a marker protein. Briefly, the immune assay plates (NUNC, Roskilde, Denmark) were coated with 5 μg/ml goat anti-human IgG antibody (MP Biomedicals, Aurora, OH) and incubated with 0.2 μg/ml of either the human TNFR1 or the human TNFR2. After blocking the non-specific binding sites, a pre-made mixture containing 100 ng/ml of wtTNF-FLAG and various concentrations of a given TNF mutant was added to the wells. After 2 h of incubation at room temperature, the wells were washed. Next, 0.5 μg/ml biotinylated anti-FLAG M2 antibody was added to each well and then the plate was incubated for an additional period of 2 h at room temperature. Wells were washed and then incubated with the horseradish peroxidase-coupled streptavidin (Zymed Lab. Inc., South San Francisco, CA) for 30 min at room temperature. The remaining bound wtTNF-FLAG was quantified as described above.

Assay for cytotoxicity mediated via TNFR1 and TNFR2. To measure cytotoxicity mediated via the TNFR1, HEp-2 cells (4×10^4 cells/well) were cultured in 96-well plates (NUNC, Roskilde, Denmark) in presence of a given TNF mutant, serially diluted human wtTNF (Peprotech, Rocky Hill, NJ), and with 100 μg/ml cycloheximide for 18 h, and cytotoxicity was assessed by using the methylene blue assay as described previously [17]. To measure cytotoxicity mediated via the TNFR2, hTNFR2/mFas-preadipocyte cells (1×10^4 cells/well) were cultured in the 96-well plates (NUNC) in presence of a given TNF mutant and serially diluted human wtTNF for 48 h, and then cell survival was determined by using the methylene blue assay.

Results and discussion

In this study, to overcome the barrier of limited transformation efficiency of *E. coli* in the preparation of high quality phage display libraries, we adopted a novel protein engineering technology in which amino acid residues at 12 different places were randomly substituted using a gene shuffling method to enhance the usefulness of the phage display technique.

Fig. 1 schematically summarizes the protocol used for constructing a novel TNF gene shuffling library. First, we prepared two phage libraries displaying mutant TNFs, in each of which six different amino acid residues (residues at positions 29, 3, 32, 145, 146 and 147 for Library I; residues at positions from 84 to 89 for Library II) present in the receptor binding site of TNF, previously identified by point mutation analysis and X-ray crystallography, were randomly substituted with other amino acid residues [11,12]. The phage libraries expressing mutant TNFs were constructed by two-step PCR as described in the Materials and methods. We confirmed that the phage Libraries I and II consisted of 8×10^6 and 6×10^6 independent clones, respectively (*data not shown*). Next, to enrich for TNFR1 binding mutants, we subjected each library to two rounds of panning using TNFR1 and recovered phage clones with high affinity to TNFR1. We used a gene shuffling method to construct the mutant TNF Shuffling Library A from these libraries, which consist of high affinity clones to TNFR1 (see Fig. 1). In the similar manner, we constructed the Shuffling Library B by carrying out panning using TNFR2. Amino acid analysis of eight randomly picked clones from each library revealed that each one of them was a mutant containing amino acid substitutions at 12 residues (*results not shown*). To concentrate TNFR1-selective mutant TNFs, the Shuffling Library A was subjected to two rounds of panning against TNFR1 using the BIAcore biosensor. After the second panning, supernatants of *E. coli* TG1 included phagemid were randomly collected and performed the screening by ELISA and bioassay to analyze their bioactivity and affinity against TNFR1 (*data not shown*). As a result, we identified six TNFR1-selective, high affinity clones, R1-15 to R1-20 (Table 1). Similarly, we identified three TNFR2-selective candidates (R2-14 to R2-16) from the Shuffling Library B (Table 1). The fact that the amino acid residue at position 87 in all active TNF receptor-selective candidates was a Tyr residue (Table 1), it suggests that Tyr87 is an important residues

Table 1
Substituted residues and affinities of TNF receptor-selective mutant candidates.

	Amino acid sequence												Relative affinity (%)[a]		
	29	31	32	84	85	86	87	88	89	145	146	147	TNFR1	TNFR2	TNFR1/TNFR2
wtTNF	L	R	R	A	V	S	Y	Q	T	A	E	S	100.0	100.0	1.0
R1-5[b]	K	A	G	–	–	–	–	–	–	–	S	T	82.0	2.0×10^{-2}	4.1×10^3
R1-15	R	N	Y	S	–	R	–	N	P	–	–	–	115.7	6.0×10^{-2}	1.9×10^3
R1-16	T	Q	Y	T	P	G	–	S	H	–	A	H	8.6	6.0×10^{-2}	1.4×10^2
R1-17	R	T	F	S	P	L	–	R	Q	S	S	T	54.2	6.0×10^{-2}	9.0×10^2
R1-18	K	N	F	S	S	H	–	T	H	–	–	–	53.9	1.0×10^{-1}	5.4×10^2
R1-19	S	N	Y	–	–	–	–	–	–	–	V	–	138.7	8.0×10^{-1}	1.7×10^3
R1-20	T	–	Y	S	H	T	–	P	S	S	Q	A	170.5	3.0×10^{-2}	5.7×10^3
R2-3[c]	–	–	–	–	–	–	–	–	–	R	–	T	<0.1	33.4	<0.0029
R2-14	–	–	–	–	P	–	–	N	S	S	A	D	1.6	103.7	0.0154
R2-15	–	–	–	S	Q	A	–	N	–	I	G	D	<0.1	141.8	<0.0007
R2-16	–	–	–	–	–	–	–	–	–	H	S	D	1.4	91.7	0.0152

Comparison of the amino acid residues of the wild-type and mutant TNFs; conserved residues are indicated using a dash.
[a] Concentration of mutant TNF required for 50% inhibition of maximal binding of wtTNF-FLAG.
[b] A TNFR1-selective mutant, which was isolated previously from the existing phage library (Library I).
[c] A TNFR2-selective mutant, which was isolated obtained from the existing phage library (Library I).

for receptor binding, which is in good agreement with the previous report [8–10].

To determine the properties of the receptor-selective candidates, we purified all the candidate TNF mutants as recombinant proteins using a general recombinant protein technology [11,12,15,18]. After each recombinant mutant TNF was expressed in *E. coli* BL21λDE3 and purified to homogeneity, we used gel electrophoresis and gel filtration chromatography to confirm that each of them, like the wtTNF, displayed MW of 17 kDa and formed a homotrimeric complex (*results not shown*). We next used a competitive ELISA to examine the binding properties of the mutant TNFs to the TNF receptors, and the results are summarized in Table 1. As summarized, all TNFR1-selective candidates showed lower affinity for TNFR2 than the wtTNF. On the other hand, affinities of the clones R1-15, R1-19, and R1-20 for TNFR1 were better than that the wtTNF. Especially, affinity of the clone R1-20 for TNFR1 was more than 1.7-fold higher than that of the wtTNF and was about 2-fold higher than that of the TNF mutant R1-5, which was previously identified from the Library I [12]. Additionally, selectivity of R1-20 for TNFR1 was higher than that of the R1-5. Next, we evaluated affinity of the TNFR2-selective mutants for TNFR2 (Table 1). Our results revealed that the clones R2-14, R2-15 and R2-16 bound to TNFR2 more strongly than the TNF mutant R2-3, which was previously isolated in our laboratory [12]. Especially, the TNF mutant R2-15 bound to TNFR2 with an affinity that was 1.4-fold higher than that of the wtTNF. R2-15 also showed superior TNFR2-selectivity than R2-3. Thus, by using the gene shuffling libraries, we were able to isolate TNF mutants that were highly receptor-selective. The receptor-selective TNF mutants R1-20 and R2-15 contained amino acid substitutions at 10 and 7 places, respectively. A point mutation analysis study of TNF suggested that the amino acid residues near position 140 are essential for TNFR1 binding [8,10,12]. In agreement with this report, we found that the residue at position 145 in the TNFR1-specific mutants is mostly retained or contained conservative amino acid substitutions, whereas more than one residues at positions 145, 146 and 147 in the TNFR2-selective mutants contained non-conservative amino acid substitutions. On the other hand, the amino acids residues near positions 30 and 80 were mostly conserved in the TNFR2-specific mutants, but not in the TNFR1-specifc mutants, suggesting that these amino acid residues might play important roles in TNFR2 binding [12]. Thus, this is the first report describing the creation of highly receptor-selective TNF mutants, namely R1-20 and R2-15, from a randomized mutant TNF library containing amino acid substitutions at 12 different amino acid residues. These results clearly demonstrate the usefulness of the developed method, which combines both phage display and gene shuffling techniques.

Next, we examined the receptor-selective bioactivities of the TNF mutants R1-20 and R2-15, each one of which showed highest receptor-selectivity, and the results are shown in Fig. 2 and Table 2. TNFR1-mediated cytotoxicity induced by the TNF mutant R1-20, as measured *in vitro* using the Hep-2 cells, was 7-fold and 2.2-fold higher than those of the mutant R1-5 and wtTNF, respectively (Fig. 2A and Table 2). Next, we evaluated the TNFR2-mediated activity of R1-20 using the hTNFR2/mFas-preadipocyte cells, which were previously constructed in our laboratory [14]. As expected, R1-20 hardly exhibited bioactivity via TNFR2, and the activity was much lower than that of the wtTNF (Fig. 2B and Table 2). On the other hand, the bioactivity of the TNFR2-selective mutant R2-15 via TNFR1 was 1000-fold lower than that of the wtTNF (Fig. 2C). The bioactivity of R2-15 via TNFR2 was, however, 2.5-fold higher than that of the wtTNF and more than 15-fold higher than that of the R2-3 mutant (Fig. 2D and Table 2). Remarkably, the bioactivity of R2-15 was higher that that of the R2-3, both of which are TNFR2-specific TNF mutants (Fig. 2D and Table 2).

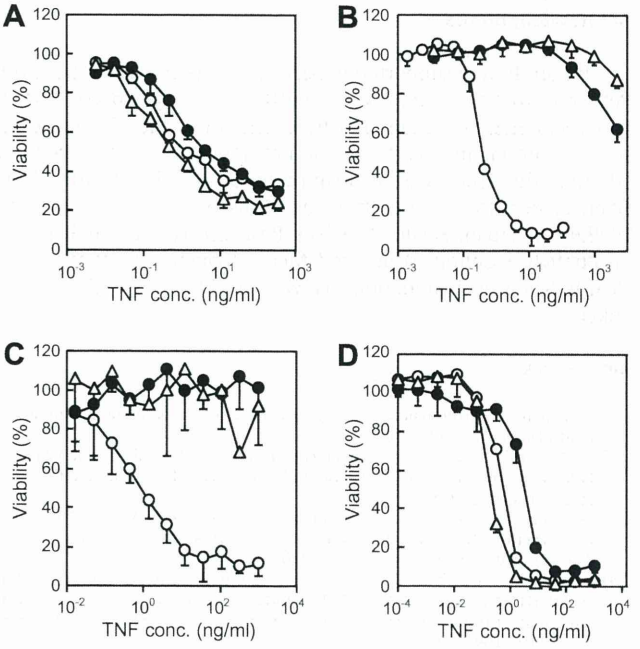

Fig. 2. Bioactivity of the receptor-selective mutants. The receptor-specific bioactivity (% viability) was measured following the treatment of HEp-2 or hTNFR2/mFas-preadipocyte cells with the wild-type or mutant TNF by using the methylene blue staining procedure as described in Materials and methods. (A) and (C) TNFR1-mediated bioactivity was measured using the HEp-2 cells. (B) and (D) TNFR2-mediated bioactivity was measured using the hTNFR2/mFas-preadipocyte cells. In (A) and (B) open circle, wtTNF; closed circle, R1-5; and open triangle, R1-20. In (C) and (D) open circle, wtTNF; closed circle, R2-3; and open triangle, R2-15.

Table 2
Bioactivity of receptor-selective mutants.

	TNFR1[a]		TNFR2[b]	
	EC50 (ng/ml)	Relative (%)	EC50 (ng/ml)	Relative (%)
wtTNF	1.3	100.0	0.4	100.0
R1-5	4.4	29.5	$>5.0 \times 10^5$	$<8.0 \times 10^{-5}$
R1-20	0.6	216.7	$>5.0 \times 10^5$	$<8.0 \times 10^{-5}$
R2-3	$>1.0 \times 10^3$	<0.1	3.1	13.0
R2-15	$>1.0 \times 10^3$	<0.1	0.2	200.0

The bioactivity values were determined from the results shown in Fig. 2 and are shown here as relative values (% wtTNF). Each value shown is mean ± SD ($n = 3$).

[a] TNFR1-mediated bioactivity was determined by a cytotoxicity assay as described in Materials and methods using the HEp-2 cells.

[b] TNFR2-mediated bioactivity was determined by a cytotoxicity assay as described in Materials and methods using the hTNFR2/mFas-preadipocyte cells.

Thus, by using the combined technology described in this study, we were able to identify TNF mutants with improved TNF receptor-selectivity and enhanced bioactivity than the existing TNF mutants.

Presently, both the underlying mechanism of signal transduction via each TNF receptor, and the relationship between the TNF receptors and onset of TNF-related diseases remain unclear. We anticipate that the TNF receptor-selective TNF mutants found in this study could be used as tools to analyze the receptor-specific signal transduction pathways. Additionally, we believe that the technology described here would be easily applicable to many disease-related proteins of unknown function. Thus, by creating structurally diverse protein libraries, we could rapidly identify therapeutically valuable proteins, which might lead to the development of effective and safe drugs in the near future.

Acknowledgments

This study was supported in part by Grants-in-Aid for Scientific Research from the Ministry of Education, Culture, Sports, Science and Technology of Japan, and by Grants-in-Aid for Scientific Research from Japan Society for the Promotion of Science (JSPS). In addition, this study was also supported in part by Health Labour Sciences Research Grants from the Ministry of Health, Labor and Welfare of Japan, Health Sciences Research Grants for Research on Publicly Essential Drugs and Medical Devices from the Japan Health Sciences Foundation, as well as The Nagai Foundation Tokyo.

References

[1] H. Wajant, K. Pfizenmaier, P. Scheurich, Tumor necrosis factor signaling, Cell Death Differ. 10 (2003) 45–65.
[2] Y. Muto, K.T. Nouri-Aria, A. Meager, G.J. Alexander, A.L. Eddleston, R. Williams, Enhanced tumour necrosis factor and interleukin-1 in fulminant hepatic failure, Lancet 2 (1988) 72–74.
[3] M. Feldmann, R.N. Maini, Lasker Clinical Medical Research Award. TNF defined as a therapeutic target for rheumatoid arthritis and other autoimmune diseases, Nat. Med. 9 (2003) 1245–1250.
[4] J. Keane, S. Gershon, R.P. Wise, E. Mirabile-Levens, J. Kasznica, W.D. Schwieterman, J.N. Siegel, M.M. Braun, Tuberculosis associated with infliximab, a tumor necrosis factor alpha-neutralizing agent, N. Engl. J. Med. 345 (2001) 1098–1104.
[5] N. Shakoor, M. Michalska, C.A. Harris, J.A. Block, Drug-induced systemic lupus erythematosus associated with etanercept therapy, Lancet 359 (2002) 579–580.
[6] T. Weiss, M. Grell, K. Siemienski, F. Muhlenbeck, H. Durkop, K. Pfizenmaier, P. Scheurich, H. Wajant, TNFR80-dependent enhancement of TNFR60-induced cell death is mediated by TNFR-associated factor 2 and is specific for TNFR60, J. Immunol. 161 (1998) 3136–3142.
[7] M. Fotin-Mleczek, F. Henkler, D. Samel, M. Reichwein, A. Hausser, I. Parmryd, P. Scheurich, J.A. Schmid, H. Wajant, Apoptotic crosstalk of TNF receptors: TNF-R2-induces depletion of TRAF2 and IAP proteins and accelerates TNF-R1-dependent activation of caspase-8, J. Cell Sci. 115 (2002) 2757–2770.
[8] X. Van Ostade, J. Tavernier, W. Fiers, Structure–activity studies of human tumour necrosis factors, Protein Eng. 7 (1994) 5–22.
[9] X.M. Zhang, I. Weber, M.J. Chen, Site-directed mutational analysis of human tumor necrosis factor-alpha receptor binding site and structure–functional relationship, J. Biol. Chem. 267 (1992) 24069–24075.
[10] J. Yamagishi, H. Kawashima, N. Matsuo, M. Ohue, M. Yamayoshi, T. Fukui, H. Kotani, R. Furuta, K. Nakano, M. Yamada, Mutational analysis of structure–activity relationships in human tumor necrosis factor-alpha, Protein Eng. 3 (1990) 713–719.
[11] H. Shibata, Y. Yoshioka, A. Ohkawa, K. Minowa, Y. Mukai, Y. Abe, M. Taniai, T. Nomura, H. Kayamuro, H. Nabeshi, T. Sugita, S. Imai, K. Nagano, T. Yoshikawa, T. Fujita, S. Nakagawa, A. Yamamoto, T. Ohta, T. Hayakawa, T. Mayumi, P. Vandenabeele, B.B. Aggarwal, T. Nakamura, Y. Yamagata, S. Tsunoda, H. Kamada, Y. Tsutsumi, Creation and X-ray structure analysis of the tumor necrosis factor receptor-1-selective mutant of a tumor necrosis factor-alpha antagonist, J. Biol. Chem. 283 (2008) 998–1007.
[12] Y. Mukai, H. Shibata, T. Nakamura, Y. Yoshioka, Y. Abe, T. Nomura, M. Taniai, T. Ohta, S. Ikemizu, S. Nakagawa, S. Tsunoda, H. Kamada, Y. Yamagata, Y. Tsutsumi, Structure–function relationship of tumor necrosis factor (TNF) and its receptor interaction based on 3D structural analysis of a fully active TNFR1-selective TNF mutant, J. Mol. Biol. 385 (2009) 1221–1229.
[13] H. Shibata, Y. Yoshioka, A. Ohkawa, Y. Abe, T. Nomura, Y. Mukai, S. Nakagawa, M. Taniai, T. Ohta, T. Mayumi, H. Kamada, S. Tsunoda, Y. Tsutsumi, The therapeutic effect of TNFR1-selective antagonistic mutant TNF-α in murine hepatitis models, Cytokine 44 (2008) 229–233.
[14] Y. Abe, T. Yoshikawa, H. Kamada, H. Shibata, T. Nomura, K. Minowa, H. Kayamuro, K. Katayama, H. Miyoshi, Y. Mukai, Y. Yoshioka, S. Nakagawa, S. Tsunoda, Y. Tsutsumi, Simple and highly sensitive assay system for TNFR2-mediated soluble- and transmembrane-TNF activity, J. Immunol. Methods 335 (2008) 71–78.
[15] Y. Yamamoto, Y. Tsutsumi, Y. Yoshioka, T. Nishibata, K. Kobayashi, T. Okamoto, Y. Mukai, T. Shimizu, S. Nakagawa, S. Nagata, T. Mayumi, Site-specific PEGylation of a lysine-deficient TNF-alpha with full bioactivity, Nat. Biotechnol. 21 (2003) 546–552.
[16] C.R. Brunetti, M. Paulose-Murphy, R. Singh, J. Qin, J.W. Barrett, A. Tardivel, P. Schneider, K. Essani, G. McFadden, A secreted high-affinity inhibitor of human TNF from Tanapox virus, Proc. Natl. Acad. Sci. USA 100 (2003) 4831–4836.
[17] Y. Tsutsumi, T. Kihira, S. Tsunoda, T. Kanamori, S. Nakagawa, T. Mayumi, Molecular design of hybrid tumour necrosis factor alpha with polyethylene glycol increases its anti-tumour potency, Br. J. Cancer 71 (1995) 963–968.
[18] H. Shibata, Y. Yoshioka, S. Ikemizu, K. Kobayashi, Y. Yamamoto, Y. Mukai, T. Okamoto, M. Taniai, M. Kawamura, Y. Abe, S. Nakagawa, T. Hayakawa, S. Nagata, Y. Yamagata, T. Mayumi, H. Kamada, Y. Tsutsumi, Functionalization of tumor necrosis factor-alpha using phage display technique and PEGylation improves its antitumor therapeutic window, Clin. Cancer Res. 10 (2004) 8293–8300.

Biomaterials 30 (2009) 5869–5876

Contents lists available at ScienceDirect

Biomaterials

journal homepage: www.elsevier.com/locate/biomaterials

The use of a mutant TNF-α as a vaccine adjuvant for the induction of mucosal immune responses

Hiroyuki Kayamuro [a,b,1], Yasuhiro Abe [a,1], Yasuo Yoshioka [a,c,1], Kazufumi Katayama [b,d], Tetsuya Nomura [a,b], Tokuyuki Yoshida [a,b], Kohei Yamashita [a,b], Tomoaki Yoshikawa [a,b], Yuichi Kawai [e], Tadanori Mayumi [e], Takachika Hiroi [d], Norio Itoh [b], Kazuya Nagano [a], Haruhiko Kamada [a,c], Shin-ichi Tsunoda [a,c,*], Yasuo Tsutsumi [a,b,c]

[a] Laboratory of Pharmaceutical Proteomics, National Institute of Biomedical Innovation (NiBio), 7-6-8 Saito-Asagi, Ibaraki, Osaka 567-0085, Japan
[b] Graduate School of Pharmaceutical Sciences, Osaka University, 1-6, Yamadaoka, Suita, Osaka 565-0871, Japan
[c] The Center for Advanced Medical Engineering and Informatics, Osaka University, 1-6, Yamadaoka, Suita, Osaka 565-0871, Japan
[d] Department of Allergy and Immunology, The Tokyo Metropolitan Institute of Medical Science, 3-18-22, Honkomagome, Bunkyo-ku, Tokyo 113-8613, Japan
[e] Faculty of Pharmaceutical Sciences, Kobe-Gakuin University, 1-1-3, Minatojima, Chuo-ku, Kobe 650-8586, Japan

ARTICLE INFO

Article history:
Received 19 May 2009
Accepted 6 July 2009
Available online 30 July 2009

Keywords:
Bioactivity
Cytokine
Mucosa
Immunomodulation

ABSTRACT

Safe and potent adjuvants are required in order to establish effective mucosal vaccines. Cytokines are promising adjuvants because they are human-derived safe biomaterial and display immune-modulating functions. We have created a mutant tumor necrosis factor-α (TNF-α), mTNF-K90R, that exhibits high bioactivity and resistance to proteases. Here, we examined the potential of mTNF-K90R as a mucosal adjuvant. Initially, we showed that intranasal co-administration of mTNF-K90R with ovalbumin (OVA) potently produced OVA-specific Immunoglobulin (Ig) G antibodies (Abs) in serum and IgA Abs both at local and distal mucosal sites compared to co-administration with wild-type TNF-α. The OVA-specific immune response was characterized by high levels of serum IgG1 and increased production of interleukin-4 (IL-4), IL-5 and IL-10 from splenocytes of immunized mice, suggesting a Th2 response. Furthermore, intranasal immunization with an antigen from influenza virus plus mTNF-K90R exhibited mucosal adjuvant activity for induction of both systemic and mucosal immune responses. Importantly, histopathological examination of the nasal tissue of mTNF-K90R treated mice detected no signs of toxicity. These findings suggest that mTNF-K90R is safe and effective mucosal adjuvant and this system may have potential application as a universal mucosal adjuvant system for mucosal vaccines improving the immune response to a variety of viral antigens.

1. Introduction

Mucosal immunity forms the first line of defense against various infectious diseases. The majority of emerging and re-emerging pathogens, including *Vibrio cholerae*, pathogenic *Escherichia coli*, HIV or influenza virus, invade and infect *via* the mucosal surfaces of the host gastrointestinal, respiratory and/or genitourinary tracts [1,2]. An important aspect of the immune response at mucosal surfaces is the production of polymeric immunoglobulin (Ig) A antibodies (Abs), as well as their transport across the epithelium and release as secretory IgA [3]. Because this IgA response represents the major mechanism for defense against viral and bacterial infections, recent efforts have been focused on the development of vaccines that are capable of inducing IgA production as well as cytotoxic T cell activation efficiently in mucosal tissues.

Mucosal vaccines administered either orally or nasally have been shown to be effective in inducing antigen-specific immune responses at both systemic and mucosal compartments [4,5]. Because of this two-layered protective immunity, mucosal vaccines are thought to be an ideal strategy for combating both emerging and re-emerging infectious diseases. However the mucosal antigen-specific immune response is weak because most protein antigens, such as non-living macromolecules or protein-subunit antigens, can evoke only a weak or undetectable adaptive immune response when they are applied mucosally [6]. Therefore, one strategy to overcome the weakness of the immune response is a co-administration of mucosal adjuvant

* Corresponding author. Laboratory of Pharmaceutical Proteomics, National Institute of Biomedical Innovation (NiBio), 7-6-8 Saito-Asagi, Ibaraki, Osaka 567-0085, Japan. Tel.: +81 72 641 9811; fax: +81 72 641 9817.
E-mail address: tsunoda@nibio.go.jp (S.-i. Tsunoda).
[1] These authors contributed equally to the work.

0142-9612/$ – see front matter © 2009 Elsevier Ltd. All rights reserved.
doi:10.1016/j.biomaterials.2009.07.009

with the vaccine antigen [4]. Unfortunately, the development of safe and effective mucosal adjuvant has proved to be challenging. As a potent mucosal vaccine adjuvant, cholera toxin (CT) or heat liable toxin have been used in experimental studies. However, the watery diarrhea induced by the administration of these toxins precludes their use as oral adjuvants in humans [7]. In addition, recent reports show that a human vaccine containing inactivated influenza and heat liable toxin as a mucosal adjuvant results in a very high incidence of Bell's palsy [8]. Therefore, development of novel mucosal vaccine adjuvants with high efficacy and safety is urgently required for clinical applications.

Cytokines are promising candidate adjuvants because they are human-derived and able to enhance the primary and memory immune responses sufficiently for protection against various infections [9–11]. One of the most important cytokines of adaptive and innate immune response is tumor necrosis factor-α (TNF-α), a proinflammatory cytokine primarily produced by T cells and macrophages [12]. TNF-α has been reported to affect certain phases of the immune process, including innate immune activation, dendritic cells (DC) maturation/recruitment, T cell activation, or pathogen clearance [13]. Indeed many reports have shown that TNF-α exerts adjuvant activities against viral infection in various model systems [14–16]. Therefore the application of TNF-α in the development of a vaccine adjuvant has been anticipated for some time. However the application of TNF-α as a mucosal vaccine adjuvant has not been reported because TNF-α administered by mucosal routes is rapidly degraded at the mucosal surface. Therefore, the maximum adjuvant effects of TNF-α are quite limited in the mucosal environment.

Previously, we have produced a bioactive lysine-deficient mutant TNF-αs from a phage library expressing mutant TNF-αs in which all of the lysine residues that act as a site of trypsin-type protease recognition were replaced with other amino acids [17–19]. Lysine-deficient mutant TNF-αs were more resistant to proteolytic cleavage than wild-type TNF-α (wTNF-α) due to the lack of lysine residues. Furthermore we demonstrated that the mTNF-K90R, one of the lysine-deficient mutant TNF-αs, showed 6-fold stronger *in vitro* bioactivity and 13-fold stronger *in vivo* bioactivity compared with wTNF-α [18].

In this study, to develop effective and safe cytokine-based mucosal vaccine adjuvants, we examined the potential of mTNF-K90R as a nasal vaccine adjuvant. We demonstrate that intranasal administration of vaccine antigen with mTNF-K90R as an adjuvant induces a strong antigen-specific systemic IgG and mucosal IgA response. In addition, the safety of mTNF-K90R was confirmed by pathological examination. These results suggest that mTNF-K90R is an attractive mucosal vaccine adjuvant for clinical application.

2. Materials and methods

2.1. Recombinant TNF-αs

wTNF-α and mTNF-K90R were prepared in house as described previously [18]. Endotoxin level was quantified using a Limulus amebocyte lysate assay kit (QCL-1000, BioWhittaker, Walkersville, MD). The endotoxin content of purified TNF-α and its mutant was <0.02 EU μg^{-1} protein.

2.2. Mice and immunization protocols

Female BALB/c mice were purchased from Nippon SLC (Kyoto, Japan) and used at 6–8 weeks of age. All of the animal experimental procedures were performed in accordance with the institutional ethical guidelines for animal experiments. Mice were intranasally immunized with a 20 μl aliquot (10 μl per nostril) containing 100 μg of ovalbumin (OVA; Sigma Chemical Co., St. Louis, MO) as antigen and 1 or 5 μg of wTNF-α or mTNF-K90R on days 0, 7 and 14. As positive control, mice were intranasally immunized with the same volume containing 100 μg of OVA and 1 μg cholera toxin B subunit (CTB; List Biological Laboratories, Campbell, CA) on days 0, 7 and 14. In the influenza virus studies, 1 μg baculovirus-expressed recombinant hemagglutinin (HA) derived from New Cal/99 virus (Protein Sciences, Meriden, CT), was immunized with 1 μg CTB or 5 μg mTNF-K90R on days 0, 7 and 14.

2.3. Sample collection

One week after the final immunization, plasma and mucosal secretions (nasal washes, saliva, vaginal washes and fecal extracts) were collected to assess antigen-specific Ab responses. Nasal and vaginal washes were collected by gentle flushing of the nasal passage or vaginal canal with 200 μl or 100 μl of sterile phosphate buffered saline (PBS), respectively. Fecal pellets (100 mg) were suspended in 1 ml of PBS and then vortexed for 30 min. The samples were centrifuged at 15 000*g* for 20 min and the supernatants were then collected as fecal extracts. Secreted saliva was collected from mice intraperitoneally injected with 0.2 mg of pilocarpine–HCl (Wako Pure Chemical Industries, Osaka, Japan).

2.4. Detection of antigen-specific Ab responses by enzyme-linked immunosorbent assay (ELISA)

Antigen-specific Ab levels in plasma, nasal washes, saliva, vaginal washes and fecal extracts were determined by ELISA. ELISA plates (Maxisorp, type 96F; Nalge Nunc International, Tokyo, Japan) were coated with 10 μg ml^{-1} OVA or 2 μg ml^{-1} HA in 0.1 M carbonate buffer and incubated overnight at 4 °C. The plates were incubated with blocking solution (Block Ace; Dainippon Sumitomo Pharmaceuticals, Osaka, Japan) at 37 °C for 2 h, and serum or mucosal secretion dilutions were added to the antigen-coated plates. After incubation at 37 °C for 2 h, the coated plates were washed with PBS–Tween 20 and incubated with a horseradish peroxidase-conjugated goat anti-mouse IgG solution or a biotin-conjugated goat anti-mouse IgA detection Ab (Southern Biotechnology Associates, Birmingham, AL) solution at 37 °C for 2 h, respectively. For detection of IgA, the plates were washed with PBS–Tween 20 and then incubated with the horseradish peroxidase-coupled streptavidin (Zymed Laboratories, South San Francisco, CA) for 1 h at RT. After incubation, the color reaction was developed with tetramethylbenzidine (MOSS, Inc. Pasadena, MD), stopped with 2 N H_2SO_4, and measured by $OD_{450-655}$ on a microplate reader.

2.5. Isolation of splenocytes

Spleens were aseptically removed and placed in RPMI 1640 (Wako Pure Chemical Industries, Osaka, Japan) supplemented with 10% fetal bovine serum, 50 μM 2-mercaptoethanol and 1% antibiotic cocktail (Nacalai tesque, Kyoto, Japan). Single-cell suspension of splenocytes was treated with ammonium chloride to lyse the red blood cells, washed, counted, and suspended in RPMI supplemented with 10% fetal bovine serum, 50 μM 2-mercaptoethanol, 1% antibiotic cocktail, 10 ml L^{-1} of a 100× nonessential amino acids solution (NEAA; Gibco-BRL), 1 mM sodium pyruvate, and 10 mM HEPES to a final concentration of 1×10^7 cells ml^{-1}.

2.6. Antigen-specific cytokine responses

Antigen-specific cytokine responses were evaluated by culturing the splenocytes (5×10^6 cells $well^{-1}$) stimulated with OVA (1 mg ml^{-1}) *in vitro*. Cells were incubated at 37 °C for 24 h (interferon-γ (IFN-γ) enzyme-linked immunospot (ELISPOT) assay), 48 h (IL-4 ELISPOT assay) or 72 h (multiplex cytokine assay).

2.7. Multiplex cytokine assay

Culture supernatants from *in vitro* unstimulated and OVA-stimulated cells were analyzed by the Bio-Plex Multiplex Cytokine Assay (Bio-Rad Laboratories, Hercules, CA) according to the manufacturer's instructions. The assay was read on a Luminex 100 (Austin, TX), and analyzed using Bio-Plex Manager software. The mean concentration of cytokines in supernatants from OVA-stimulated cells over the unstimulated background was then calculated.

2.8. Cytokine ELISPOT assay

An ELISPOT assay was performed to detect IFN-γ and IL-4 producing cells. After 24 h (IFN-γ) or 48 h (IL-4) incubation at 37 °C, the plate was washed, and the IFN-γ and IL-4 producing cells were measured by an ELISPOT assay kit (BD Biosciences), according to the manufacturer's instructions.

2.9. Fluorescence microscopy

BALB/c mice were administered intranasally with fluorescent isothiocyanate (FITC) labeled OVA (FITC-OVA; Molecular Probes–Invitrogen, Eugene, OR) at 50 μg $mouse^{-1}$ with or without mTNF-K90R (5 μg $mouse^{-1}$). After 15 min, the heads of the anesthetized mice were severed from the body. The heads were placed in fixative solution, and embedded in OCT compound (Sakura FineTek Japan Co. Ltd., Tokyo, Japan) and frozen tissue sections were prepared. FITC-OVA was observed under fluorescence microscopy (×20).

2.10. Histopathological analysis

For three times immunization protocol, BALB/c mice were immunized with OVA with or without mTNF-K90R at a dose of 1 μg, 5 μg or 25 μg on days 0, 7 and 14.

Seven days after the last immunization, heads of the mice were severed from the body and then placed in fixative solution (4% paraformaldehyde). Histopathological examination was performed by the Applied Medical Research Laboratory (Osaka, Japan). For single immunization protocol, BALB/c mice were immunized with OVA with or without mTNF-K90R at a dose of 5 μg. At 2 h after single immunization, histopathological examination was performed using the same protocol.

2.11. Statistical analysis

All results are expressed as mean ± SEM. Statistical significance in differences were evaluated by Newman–Keuls Multiple Comparison Test after analysis of variance (ANOVA).

3. Results

3.1. Mucosal adjuvant activity of mTNF-K90R

To examine the properties of mTNF-K90R as a mucosal vaccine adjuvant, mice were intranasally immunized with 100 μg OVA plus wTNF-α (1 μg mice^{-1}), mTNF-K90R (1 μg mice^{-1}, 5 μg mice^{-1}), or CTB (1 μg mice^{-1}) three times at weekly intervals. Seven days after the last immunization, we examined the level of anti-OVA Abs response in the serum by ELISA (Fig. 1A). Intranasal immunization with OVA plus 1 μg mTNF-K90R induced higher levels of anti-OVA IgG Ab response in serum than after immunization with OVA alone or OVA plus 1 μg wTNF-α. Furthermore, OVA-specific IgG Ab levels of mTNF-K90R immunized mice were of a similar magnitude to those immunized with CTB, a common laboratory mucosal adjuvant.

Serum IgG subclass responses have been used to assess the type of immune response elicited by immunization. For example, IgG1 is indicative of a Th2-type response whereas IgG2a is indicative of a Th1-type response. To assess the type of immune response induced by mTNF-K90R, serum OVA-specific IgG subclass responses were also examined (Fig. 1B). OVA-specific IgG1 Ab levels of 1 μg mTNF-K90R immunized mice were higher than those immunized with OVA alone or OVA plus 1 μg wTNF-α, and as well as in mice immunized with CTB. However, the level of OVA-specific IgG2a was low in all groups, indicating that mTNF-K90R may induce immune responses with an antigen-specific Th2 component.

Next, we examined the OVA-specific IgA secretion in nasal washes, vaginal washes, and fecal extracts from immunized mice (Fig. 2). As expected, immunization with OVA plus CTB induced strong anti-OVA IgA secretion in all mucosal tissues. Nasal immunization with OVA plus 1 μg of mTNF-K90R tended to induce high levels of OVA-specific IgA secretion in nasal tissue and fecal extract compared with after immunization with OVA plus 1 μg wTNF-α. The IgA level of 1 μg mTNF-K90R immunized mice in nasal tissue was of a similar magnitude to those immunized with CTB. In contrast, the IgA level in vaginal tissue and fecal extract was lower for the 1 μg mTNF-K90R treated mice compared with that of CTB treated mice. Nasal immunization with OVA plus 5 μg of mTNF-K90R induced high OVA-specific IgA secretion in multiple mucosal tissues compared to 1 μg of mTNF-K90R and comparable anti-OVA Abs responses to those induced with OVA plus CTB. These results indicate that mTNF-K90R is an attractive mucosal vaccine adjuvant for the induction of antigen-specific systemic IgG and mucosal IgA responses.

3.2. Antigen-specific cytokine responses of mTNF-K90R

To clarify the mechanism of immune response elicited by mTNF-K90R, the release profiles of cytokines from splenocytes of OVA-immunized mice were analyzed. Culture supernatants from

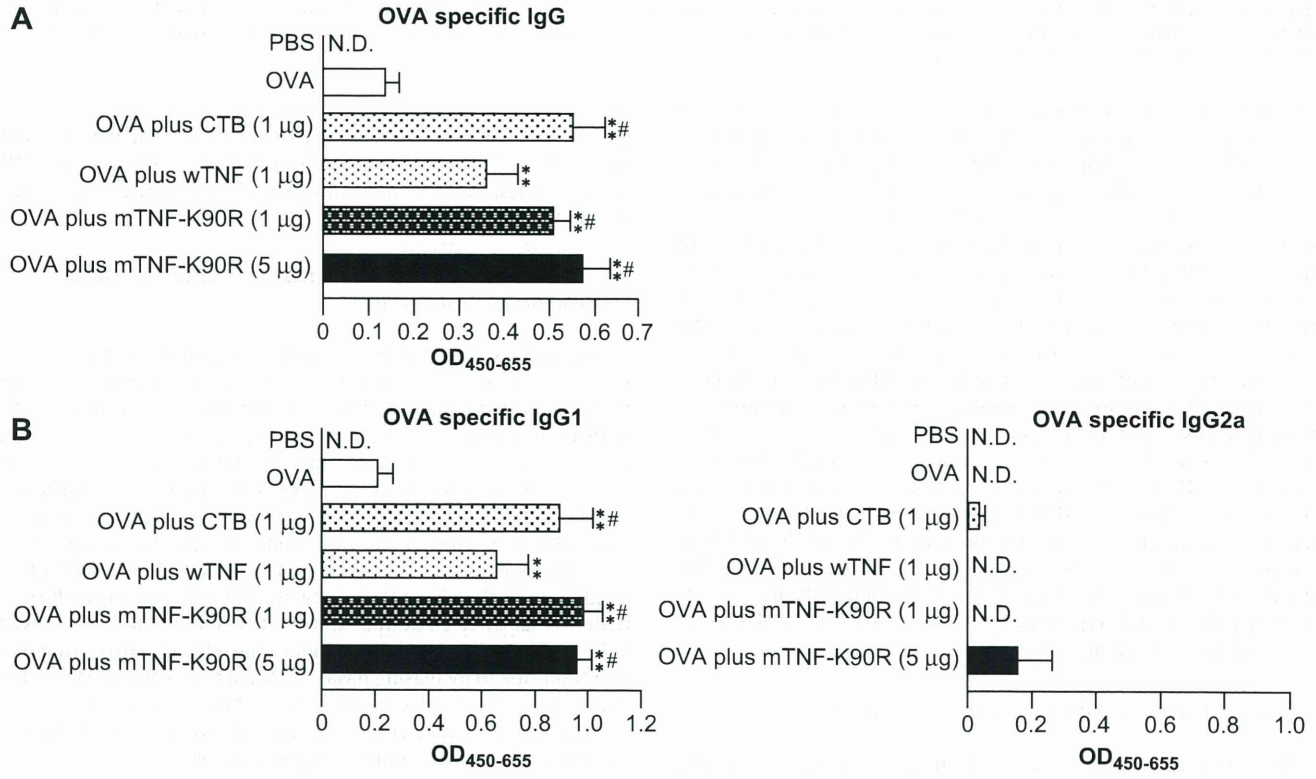

Fig. 1. Serum OVA-specific IgG Abs response after nasal immunization with OVA plus adjuvant. BALB/c mice were intranasally immunized with OVA alone, OVA plus 1 μg CTB, OVA plus 1 μg wTNF-α, OVA plus 1 μg mTNF-K90R or OVA plus 5 μg mTNF-K90R once a week for three consecutive weeks. Serum was collected 1 wk after the last immunization and analyzed by ELISA for OVA-specific IgG (A) and IgG subclass (B) at a 1:100 dilution of serum. Data represents the mean of absorbance 450 nm (reference wave, 655 nm). N.D; not detected. Data are presented as means ± SEM ($n = 7$; $^{**}P < 0.01$ *versus* value for OVA alone treated group by ANOVA; $^{\#}P < 0.05$ *versus* value for OVA plus wTNF-α treated group by ANOVA).

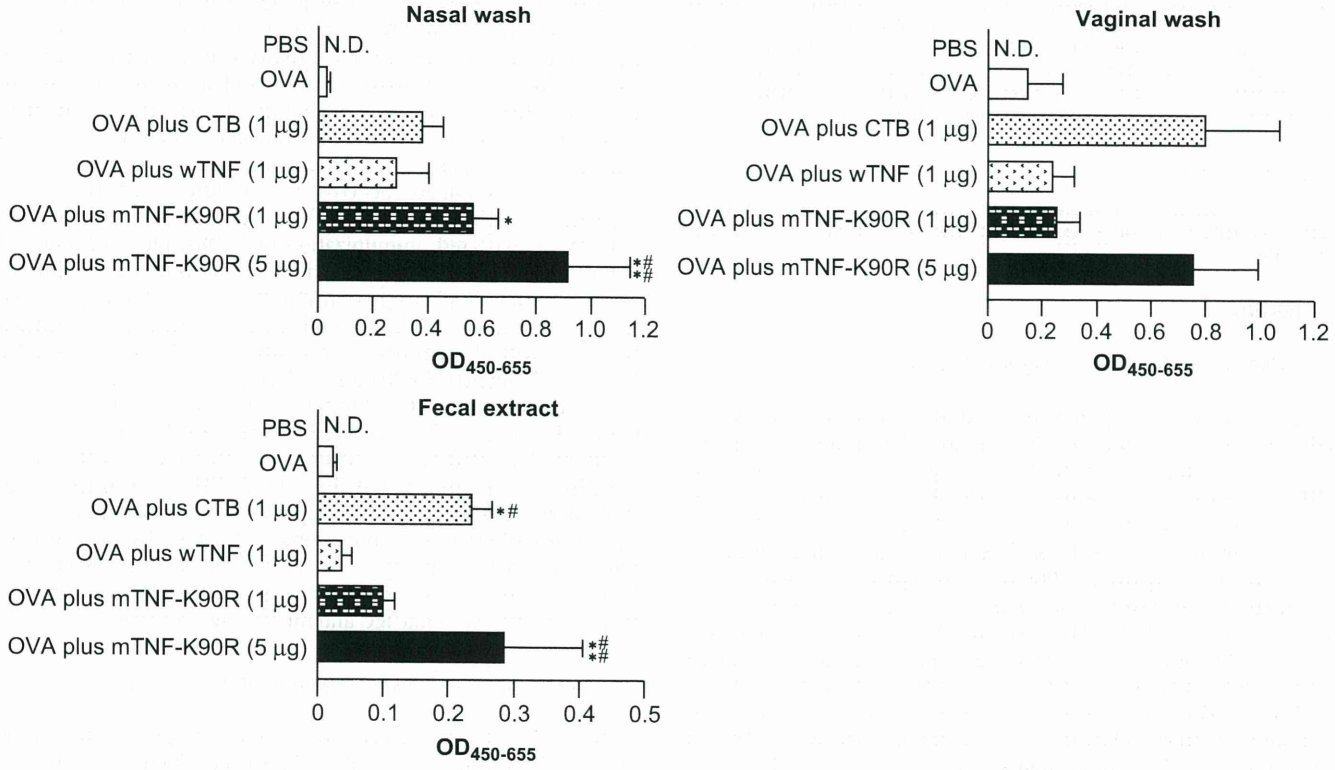

Fig. 2. OVA-specific mucosal IgA Abs response after nasal immunization with OVA plus adjuvant. BALB/c mice were intranasally immunized with OVA alone, OVA plus 1 μg CTB, OVA plus 1 μg wTNF-α, OVA plus 1 μg mTNF-K90R or OVA plus 5 μg mTNF-K90R once a week for three consecutive weeks. Mucosal secretions were collected 1 wk after the last immunization and OVA-specific IgA Abs responses in nasal wash, vaginal wash and fecal extract were determined by ELISA at a 1:8 dilution. Data represents the mean of absorbance 450 nm (reference wavelength, 655 nm). Data are presented as means ± SEM ($n = 7$; $^{*}P < 0.05$, $^{**}P < 0.01$ *versus* value for OVA alone treated group by ANOVA; $^{\#}P < 0.05$, $^{\#\#}P < 0.01$ *versus* value for OVA plus wTNF-α treated group by ANOVA).

OVA-stimulated splenocytes collected from immunized mice were assessed for Th2-type cytokines IL-4, IL-5, IL-10, granulocyte macrophage colony-stimulating factor (GM-CSF) (Fig. 3A) and Th1-type cytokines IL-12 and IFN-γ (Fig. 3B), using a multiplexed immunobeads assay. Splenocytes from mice immunized with OVA plus 1 μg mTNF-K90R exhibited higher levels of Th2-type cytokines (IL-4, IL-5, IL-10 and GM-CSF) than those responses induced with OVA plus 1 μg wTNF-α or CTB (Fig. 3A). In contrast, there was hardly any difference in Th1-type cytokine (IL-12 and IFN-γ) secretion amongst all of the immunized mice (Fig. 3B). To further characterize the type of immune response, the level of OVA-specific IFN-γ and IL-4-secreting splenocytes from OVA-immunized mice with the various adjuvants was determined using a cytokine-specific ELISPOT assay (Fig. 4). The level of OVA-specific IL-4-secreting splenocytes from OVA-immunized mice with mTNF-K90R was greater than those responses observed after administration of wTNF-α or CTB. By contrast, the level of IFN-γ-secreting splenocytes in OVA-immunized mice with mTNF-K90R was no different from the levels observed for mice immunized with OVA alone. These results suggested that mTNF-K90R induced a more strongly polarized Th2-type immune response when mTNF-K90R was used as a mucosal vaccine adjuvant.

3.3. Mucosal adjuvant efficacy against influenza virus

We anticipated that a mucosal influenza virus-neutralizing antibody response would generate an ideal vaccine against these infectious diseases. To estimate the mucosal adjuvant efficacy of mTNF-K90R for influenza virus HA vaccine, the antibody response against HA was examined in mice intranasally immunized with mTNF-K90R (Fig. 5). Mice receiving HA plus 5 μg of mTNF-K90R induced a significantly greater anti-HA IgG or IgA response in serum, saliva or nasal wash compared with mice receiving HA alone or HA plus CTB. These results indicated that application of mTNF-K90R as a nasal vaccine adjuvant to viral infectious diseases might be an effective strategy.

3.4. Localization of antigens into nasopharyngeal-associated lymphoreticular tissue (NALT)

Because NALT plays an important role in the initial induction of the mucosal immune response, it was important to determine the tissue localization of the antigens. To characterize the mechanism of mTNF-K90R in the induction of OVA-specific mucosal and systemic immune responses, we examined the localization of OVA in NALT derived from mice that were immunized with OVA in the absence or presence of mTNF-K90R (Fig. 6). Fluorescence microscopic analysis revealed that FITC-OVA was mainly located beneath the nasal epithelium surrounding NALT in mice treated with FITC-OVA alone. By contrast, in addition to the subepithelial region, FITC-OVA was also observed within NALT after co-administration of mTNF-K90R. These results indicate that mTNF-K90R might induce the effective entry of antigens into NALT due to increasing nasal epithelial permeability. We believe that the observed response of mTNF-K90R in the nasal epithelial reflects one of the mechanisms for the induction of antigen-specific mucosal and systemic immune response in mice.

3.5. Safety examination of mTNF-K90R

While enterotoxin-based adjuvants display a strong mucosal response, they also induce severe central nervous system damage

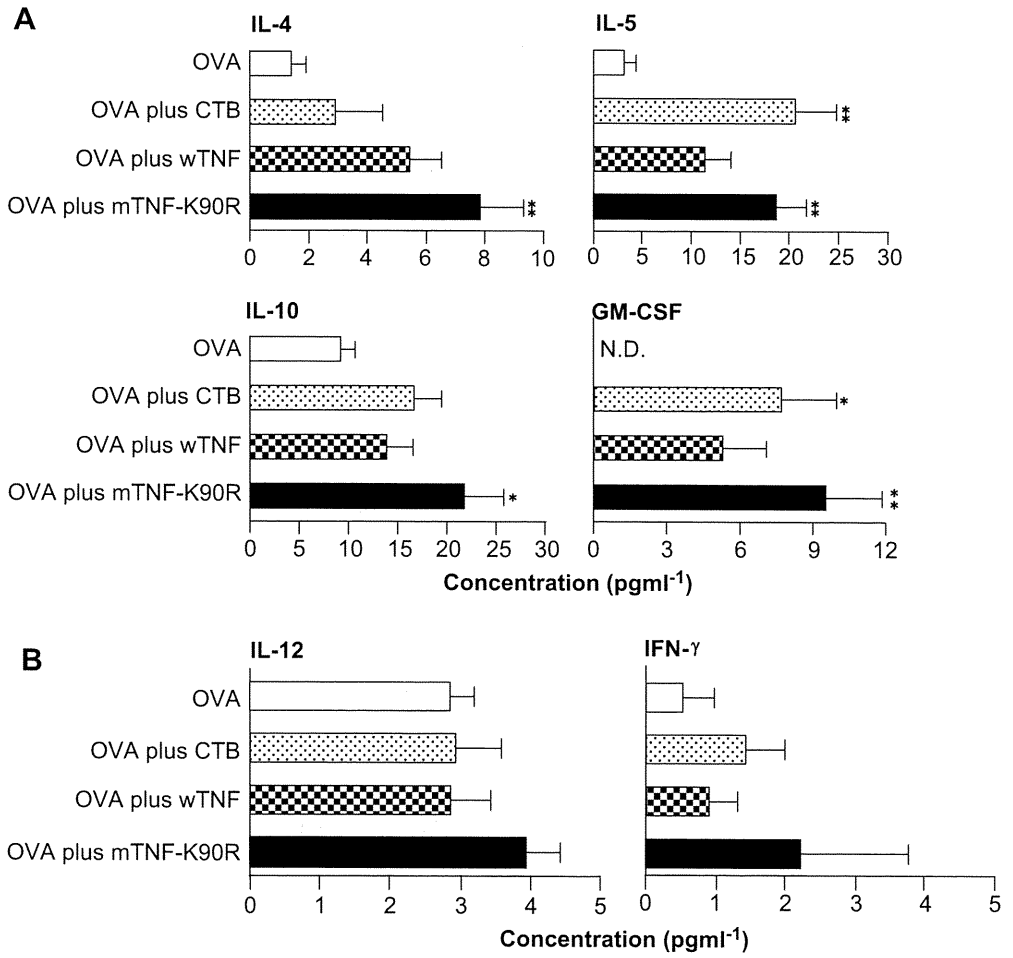

Fig. 3. Cytokine response induced after nasal immunization with OVA plus adjuvant. BALB/c mice were intranasally immunized with OVA alone, OVA plus 1 μg CTB, OVA plus 1 μg wTNF-α or OVA plus 1 μg mTNF-K90R once a week for three consecutive weeks. One week after the last immunization, splenocytes from each group were cultured with 1 mg ml^{-1} OVA. Culture supernatants were harvested following 3 days of incubation, and OVA-specific Th2-type (A) and Th1-type (B) cytokine productions in culture supernatant were analyzed by using the Bio-Plex Multiplex Cytokine Assay. Data are presented as means ± SEM ($n = 6$; $^{*}P < 0.05$, $^{**}P < 0.01$ *versus* value for OVA alone treated group by ANOVA).

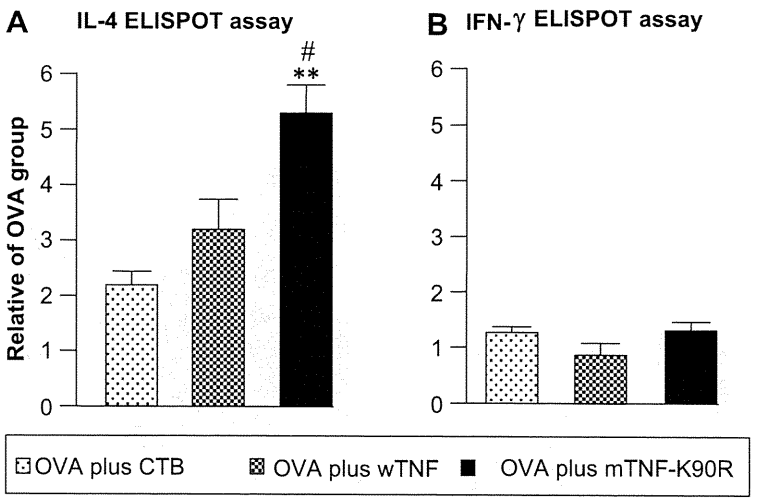

Fig. 4. Analysis of OVA-specific cytokine-secreting cells in mice nasally immunized with OVA plus adjuvant. BALB/c mice were intranasally immunized with OVA alone, OVA plus 1 μg CTB, OVA plus 1 μg wTNF-α or OVA plus 1 μg mTNF-K90R once a week for three consecutive weeks. One week after the last immunization, splenocytes from each group were cultured with 1 mg ml^{-1} OVA. The levels of OVA-specific IL-4 (a) and IFN-γ-producing cells (b) were examined by individual cytokine-specific ELISPOT assay. Data are presented as means ± SEM ($n = 3$; $^{**}P < 0.01$ *versus* value for OVA plus CTB treated group by ANOVA; $^{\#}P < 0.05$ *versus* value for OVA plus wTNF-α treated group by ANOVA).

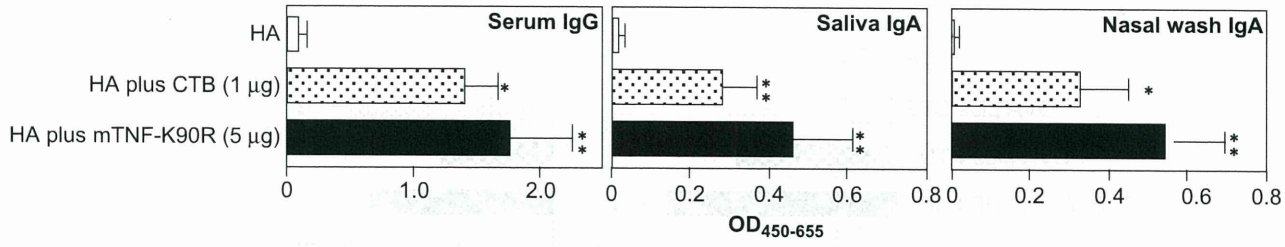

Fig. 5. mTNF-K90R induced mucosal IgA and IgG responses against influenza virus HA in mice. BALB/c mice were immunized intranasally with HA together with 1 μg CTB or 5 μg mTNF-K90R. One week after the last immunization, HA-specific IgG in serum at a 1:500 dilution and IgA in nasal or saliva at a 1:8 dilution were assessed by ELISA at a 1:8 dilution. Data represents the mean of absorbance 450 nm (reference wavelength, 655 nm). N.D; not detected. Data are presented as means ± SEM ($n = 4$–6; $^{*}P < 0.05$, $^{**}P < 0.01$ *versus* value for HA alone treated group by ANOVA).

due to the presence of a specific receptor, GM1 ganglioside, which is highly expressed in neuronal tissue [20]. This neurotoxicity has severely restricted the use enterotoxins as adjuvants for mucosal vaccines in clinical practice. To evaluate the *in vivo* toxicity of mTNF-K90R, inflammatory response and tissue injury were assessed in the nasal tissue (Fig. 7). Tissue sections of the nasal cavity were prepared at various time points after immunization of OVA plus mTNF-K90R. However, no tissue injury could be detected in any of the sections. These observations indicate no membrane barrier disruption and/or inflammatory changes, not even after 2 h single immunization with 5 μg mTNF-K90R (Fig. 7A and B). Furthermore, increasing the dose of mTNF-K90R given intranasally from 1 μg to 25 μg did not seem to have an adverse effect on the mice after three immunizations (Fig. 7C and D). Thus, although further evaluation is required, the results of this initial study demonstrated that the toxicity of mTNF-K90R is likely to be relatively low.

4. Discussion

In this study, we examined the mucosal adjuvant activity of mTNF-K90R and showed that intranasal co-administration of mTNF-K90R with antigen strongly induced both antigen-specific IgG in serum and IgA at mucosal site (nasal cavity, oral cavity, vagina and intestine). The enhanced adjuvant effect of mTNF-K90R might be caused by improved bioactivity and protease resistance compared to wTNF-α. Although mTNF-K90R showed a potent adjuvant effect on mucosal immunity, it does not elicit excessive inflammatory symptoms, such as formation of edema or fibrosis. Therefore, we believe that mTNF-K90R is a potent mucosal adjuvant for vaccines against various infectious diseases.

The development of a safe and effective vaccine is critical in preventing the spread of influenza virus. It is generally thought that or anti-influenza virus-neutralizing antibody must be induced at mucosal surfaces in order to prevent influenza virus infection. Previous studies also reported that antigen-specific systemic IgG and mucosal IgA Abs have potentially important roles for protection against the influenza virus [21,22]. Therefore, our results suggest that mTNF-K90R might be a superior mucosal vaccine adjuvant against infectious diseases caused by influenza virus.

TNF-α is anticipated to be used as a therapeutic drug to treat cancer. TNF-α has been used clinically for the treatment of non-resectable high-grade sarcoma and melanoma by locoregional applications in combination with melphalan under the approval of the European Agency for the Evaluation of Medicinal Products because systemic administration of TNF-α at therapeutically effective doses is limited by its unacceptable toxic side effects [23,24]. Further, in a recent report, it has been suggested that TNF-α had the potentials of the genetic toxicity, because TNF-α caused DNA damage through its ability to induce reactive oxygen species [25]. Thus, it is important to examine the safety of mTNF-K90R in a protocol using a mucosal vaccine adjuvant. Previously, we reported that mTNF-K90R had 1.3-fold lower *in vivo* toxicity after systemic administration compared with that of wTNF-α because of a change in the pharmacokinetics. Similarly, no adverse effect on the nasal mucosa was observed in this study after intranasal administration of mTNF-K90R. Although detailed examinations are required, mTNF-K90R is expected to be a useful mucosal vaccine adjuvant. Furthermore, we have shown that conjugating cytokines with polyethylene glycol (PEG) improves their safety *in vivo* [17,18,26–28]. We have also developed a novel site-specific PEGylation process to overcome the

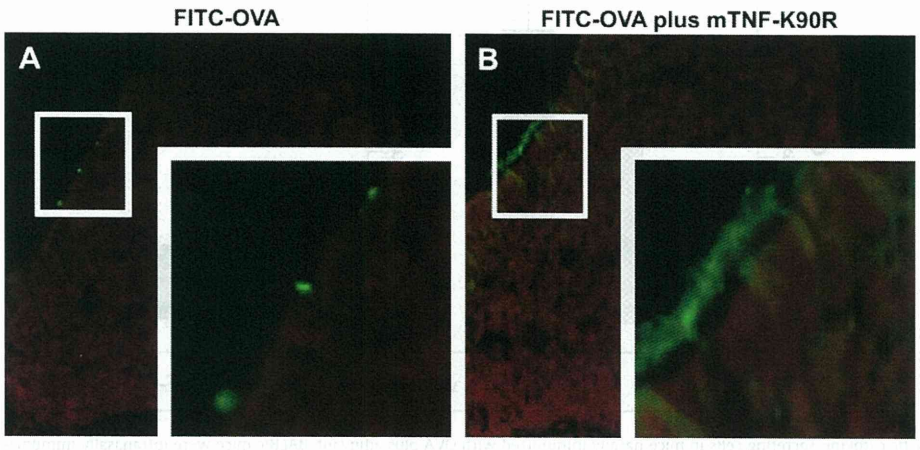

Fig. 6. Localization analysis of OVA in NALT. BALB/c mice were administered 50 μg FITC-OVA and a combination of 5 μg mTNF-K90R as a nasal vaccine adjuvant. Frozen sections of NALT resected from mice treated with FITC-OVA alone (A) and a combination of mTNF-K90R (B). The FITC-OVA (green) signals were detected by fluorescence microscopy. The nucleus was counterstained using PI (red). The original magnification of these photographs was 20×.

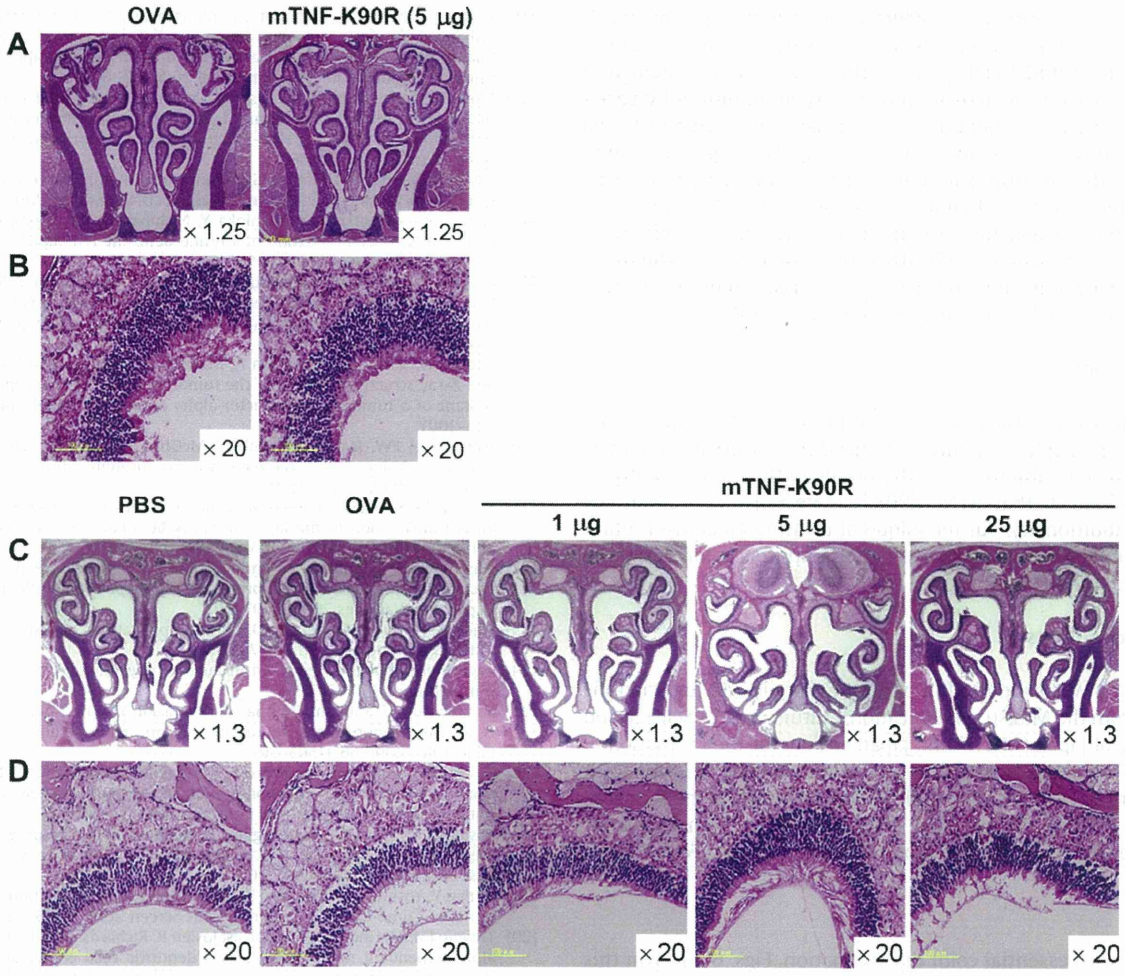

Fig. 7. Histopathological analysis of nasal cavity treated with mTNF-K90R. Frontal cross-sections of the nasal cavity from mice, taken 2 h after administration (A, B) or one week after three times administration of PBS, OVA alone, and OVA together with 1 μg, 5 μg or 25 μg mTNF-K90R (C, D). An overall view of the nasal passage is shown in (A) and (C). The region of nasal olfactory epithelia is shown in (B) and (D). Sections were prepared and the tissues were stained with H&E to assess the degree of tissue injury and local inflammation.

problems of PEGylation [17,18,26,28]. Previously we showed that the application of this technology to mTNF-K90R improved the safety and the anti-tumor effects of mTNF-K90R [18]. We are currently examining the safety and efficacy of site-specific PEGylated mTNF-K90R as a mucosal vaccine adjuvant.

The effects of mTNF-K90R at mucosal tissue was also analyzed. We reasoned that the adjuvant effect of mTNF-K90R may be related to its stimulation of antigen-presenting cells, such as DC. Indeed, DC plays a crucial role in eliciting T cell-dependent immunity. TNF-α is known to have profound effects on DC function and contributing to their activation, maturation and migration to, and accumulation within, draining lymph nodes [29,30]. Moreover, DC stimulated by TNF-α prior to anti-tumor vaccination or transfection with the TNF-α gene are reported to induce anti-tumor immunity [14,15]. However, we found that mTNF-K90R significantly enhanced the permeability of the nasal epithelial layer and diffusion of antigen into NALT. Consistent with our results, some reports have shown that TNF-α causes an increase in intestinal permeability [25,31]. Taken together, these results suggest that the strong mucosal adjuvant activity of mTNF-K90R is caused, at least in part, by increased epithelial permeability. In addition, TNF-α causes up-regulation of human polymeric Ig receptor on mucosal epithelial cells [32]. Polymeric Ig receptor transports polymeric IgA into external secretions as secretory IgA, which is critical for the defense of mucosal tissues [33]. We believe that multiple actions of mTNF-K90R contribute to its potent adjuvant activity. Currently, we are attempting to elucidate these various mechanisms.

Induction of both Th1- and Th2-type responses is the major goal for the development of mucosal vaccines because these responses would provide protective immunity against viral and bacterial infections by maximizing antigen-specific Ab and cytolytic T lymphocytes (CTL) responses. Although mTNF-K90R is not likely to induce CTLs, it could efficiently induce Abs responses. To induce both antigen-specific Ab and CTL responses, combinatorial administration of mTNF-K90R with another mucosal adjuvant, which can induce Th1-type immune responses, is applicable. We have already screened the TNF superfamily and other cytokines and succeeded in finding candidates that can effectively induce CTL at the mucosal site. The combinatorial effect of the cytokines and mTNF-K90R as a mucosal vaccine adjuvant is now under examination.

Recently, vaccine therapy has been attempted not only to combat cancer or viral infections but also for other diseases such as Alzheimer-type dementia. Schenk et al. demonstrated that intraperitoneal vaccination of β-amyloid peptide plus Freund's adjuvant to a murine Alzheimer's disease model resulted in a dramatic reduction of cerebral amyloidosis [34]. This therapeutic approach is clearly efficacious; however, the safety of this strategy is of paramount importance. In a clinical trial, approximately 6% of patients

administered a synthetic β-amyloid peptide plus adjuvant developed aseptic meningoencephalitis, most likely mediated by brain-infiltrating activated T cells [35,36]. This adverse effect seemed to be associated with the activation of Th1-type immunity by vaccination with β-amyloid peptide [37,38]. Nikolic et al. demonstrated that immunization capable of inducing Th2-type immunity predominantly constitutes an effective and potentially safe treatment strategy for Alzheimer's disease [39]. Therefore, our mTNF-K90R is a promising development in the establishment of an easy-to-use, efficacious, safe immunotherapy for Alzheimer's disease. However, further analyses are necessary in order to elucidate the Th2-dominant mechanism of mTNF-K90R.

5. Conclusions

In summary, our study showed that mTNF-K90R, engineered by using a phage display technique, induced two layers of protective immunity when administered intranasally with a vaccine antigen. Our results indicate that mTNF-K90R is a safe and effective mucosal adjuvant. Additionally, our technique of creating bioactive mutant cytokines might be an attractive generic approach for designing novel mucosal adjuvants.

Acknowledgements

This study was supported in part by Grants-in-Aid for Scientific Research from the Ministry of Education, Culture, Sports, Science and Technology of Japan (MEXT) and Japan Society for the Promotion of Science (JSPS), some Health Labour Sciences Research Grants from the Ministry of Health, Labor, and Welfare in Japan by the Research on Health Sciences focusing on Drug Innovation from the Japan Health Sciences Foundation and by the Takeda Science Foundation.

Appendix

Figures with essential color discrimination. Figs. 6 and 7 in this article may be difficult to interpret in black and white. The full color images can be found in the on-line version, at doi:10.1016/j.biomaterials.2009.07.009.

References

[1] Eriksson K, Holmgren J. Recent advances in mucosal vaccines and adjuvants. Curr Opin Immunol 2002;14:666–72.
[2] Haynes BF, Shattock RJ. Critical issues in mucosal immunity for HIV-1 vaccine development. J Allergy Clin Immunol 2008;122:3–9.
[3] Brandtzaeg P. Induction of secretory immunity and memory at mucosal surfaces. Vaccine 2007;25:5467–84.
[4] Holmgren J, Czerkinsky C. Mucosal immunity and vaccines. Nat Med 2005;11:S45–53.
[5] Neutra MR, Kozlowski PA. Mucosal vaccines: the promise and the challenge. Nat Rev Immunol 2006;6:148–58.
[6] Ada G. Vaccines and vaccination. N Engl J Med 2001;345:1042–53.
[7] Gorbach SL, Khurana CM. Toxigenic *Escherichia coli* in infantile diarrhea in Chicago. J Lab Clin Med 1971;78:981–2.
[8] Mutsch M, Zhou W, Rhodes P, Bopp M, Chen RT, Linder T, et al. Use of the inactivated intranasal influenza vaccine and the risk of Bell's palsy in Switzerland. N Engl J Med 2004;350:896–903.
[9] Boyaka PN, Marinaro M, Jackson RJ, Menon S, Kiyono H, Jirillo E, et al. IL-12 is an effective adjuvant for induction of mucosal immunity. J Immunol 1999;162:122–8.
[10] Staats HF, Bradney CP, Gwinn WM, Jackson SS, Sempowski GD, Liao HX, et al. Cytokine requirements for induction of systemic and mucosal CTL after nasal immunization. J Immunol 2001;167:5386–94.
[11] Toka FN, Pack CD, Rouse BT. Molecular adjuvants for mucosal immunity. Immunol Rev 2004;199:100–12.
[12] Wajant H, Pfizenmaier K, Scheurich P. Tumor necrosis factor signaling. Cell Death Differ 2003;10:45–65.
[13] Calzascia T, Pellegrini M, Hall H, Sabbagh L, Ono N, Elford AR, et al. TNF-alpha is critical for antitumor but not antiviral T cell immunity in mice. J Clin Invest 2007;117:3833–45.
[14] Brunner C, Seiderer J, Schlamp A, Bidlingmaier M, Eigler A, Haimerl W, et al. Enhanced dendritic cell maturation by TNF-alpha or cytidine-phosphate-guanosine DNA drives T cell activation *in vitro* and therapeutic anti-tumor immune responses in vivo. J Immunol 2000;165:6278–86.
[15] Chen Z, Huang H, Chang T, Carlsen S, Saxena A, Marr R, et al. Enhanced HER-2/neu-specific antitumor immunity by cotransduction of mouse dendritic cells with two genes encoding HER-2/neu and alpha tumor necrosis factor. Cancer Gene Ther 2002;9:778–86.
[16] Nimal S, Heath AW, Thomas MS. Enhancement of immune responses to an HIV gp120 DNA vaccine by fusion to TNF alpha cDNA. Vaccine 2006;24:3298–308.
[17] Yamamoto Y, Tsutsumi Y, Yoshioka Y, Nishibata T, Kobayashi K, Okamoto T, et al. Site-specific PEGylation of a lysine-deficient TNF-alpha with full bioactivity. Nat Biotechnol 2003;21:546–52.
[18] Shibata H, Yoshioka Y, Ikemizu S, Kobayashi K, Yamamoto Y, Mukai Y, et al. Functionalization of tumor necrosis factor-alpha using phage display technique and PEGylation improves its antitumor therapeutic window. Clin Cancer Res 2004;10:8293–300.
[19] Shibata H, Yoshioka Y, Ohkawa A, Minowa K, Mukai Y, Abe Y, et al. Creation and X-ray structure analysis of the tumor necrosis factor receptor-1-selective mutant of a tumor necrosis factor-alpha antagonist. J Biol Chem 2008;283:998–1007.
[20] van Ginkel FW, Jackson RJ, Yuki Y, McGhee JR. Cutting edge: the mucosal adjuvant cholera toxin redirects vaccine proteins into olfactory tissues. J Immunol 2000;165:4778–82.
[21] Veazey RS, Shattock RJ, Pope M, Kirijan JC, Jones J, Hu Q, et al. Prevention of virus transmission to macaque monkeys by a vaginally applied monoclonal antibody to HIV-1 gp120. Nat Med 2003;9:343–6.
[22] Hasegawa H, Ichinohe T, Tamura S, Kurata T. Development of a mucosal vaccine for influenza viruses: preparation for a potential influenza pandemic. Expert Rev Vaccines 2007;6:193–201.
[23] Lejeune FJ, Ruegg C, Lienard D. Clinical applications of TNF-alpha in cancer. Curr Opin Immunol 1998;10:573–80.
[24] Eggermont AM. TNF registered in Europe: does TNF get a second chance? J Immunother 2000;23:505–6.
[25] Yan B, Wang H, Rabbani ZN, Zhao Y, Li W, Yuan Y. Tumor necrosis factor-alpha is a potent endogenous mutagen that promotes cellular transformation. Cancer Res 2006;66:11565–70.
[26] Yoshioka Y, Tsutsumi Y, Ikemizu S, Yamamoto Y, Shibata H, Nishibata T, et al. Optimal site-specific PEGylation of mutant TNF-alpha improves its antitumor potency. Biochem Biophys Res Commun 2004;315:808–14.
[27] Yoshioka Y, Tsutsumi Y, Nakagawa S, Mayumi T. Recent progress on tumor missile therapy and tumor vascular targeting therapy as a new approach. Curr Vasc Pharmacol 2004;2:259–70.
[28] Mukai Y, Yoshioka Y, Tsutsumi Y. Phage display and PEGylation of therapeutic proteins. Comb Chem High Throughput Screen 2005;8:145–52.
[29] Trevejo JM, Marino MW, Philpott N, Josien R, Richards EC, Elkon KB, et al. TNF-alpha-dependent maturation of local dendritic cells is critical for activating the adaptive immune response to virus infection. Proc Natl Acad Sci U S A 2001;98:12162–7.
[30] Lee LF, Xu B, Michie SA, Beilhack GF, Warganich T, Turley S, et al. The role of TNF-alpha in the pathogenesis of type 1 diabetes in the nonobese diabetic mouse: analysis of dendritic cell maturation. Proc Natl Acad Sci U S A 2005;102:15995–6000.
[31] Gitter AH, Bendfeldt K, Schmitz H, Schulzke JD, Bentzel CJ, Fromm M. Epithelial barrier defects in HT-29/B6 colonic cell monolayers induced by tumor necrosis factor-alpha. Ann N Y Acad Sci 2000;915:193–203.
[32] Takenouchi-Ohkubo N, Moro I, Mukae S, Kaneko Y, Komiyama K. Tumour necrosis factor-alpha-mediated human polymeric immunoglobulin receptor expression is regulated by both mitogen-activated protein kinase and phosphatidylinositol-3-kinase in HT-29 cell line. Immunology 2008;123:500–7.
[33] Mestecky J, McGhee JR. Immunoglobulin A (IgA): molecular and cellular interactions involved in IgA biosynthesis and immune response. Adv Immunol 1987;40:153–245.
[34] Schenk D, Barbour R, Dunn W, Gordon G, Grajeda H, Guido T, et al. Immunization with amyloid-beta attenuates Alzheimer-disease-like pathology in the PDAPP mouse. Nature 1999;400:173–7.
[35] Hock C, Konietzko U, Streffer JR, Tracy J, Signorell A, Muller-Tillmanns B, et al. Antibodies against beta-amyloid slow cognitive decline in Alzheimer's disease. Neuron 2003;38:547–54.
[36] Bayer AJ, Bullock R, Jones RW, Wilkinson D, Paterson KR, Jenkins L, et al. Evaluation of the safety and immunogenicity of synthetic Abeta42 (AN1792) in patients with AD. Neurology 2005;64:94–101.
[37] Nicoll JA, Wilkinson D, Holmes C, Steart P, Markham H, Weller RO. Neuropathology of human Alzheimer disease after immunization with amyloid-beta peptide: a case report. Nat Med 2003;9:448–52.
[38] Monsonego A, Imitola J, Petrovic S, Zota V, Nemirovsky A, Baron R, et al. Abeta-induced meningoencephalitis is IFN-gamma-dependent and is associated with T cell-dependent clearance of Abeta in a mouse model of Alzheimer's disease. Proc Natl Acad Sci U S A 2006;103:5048–53.
[39] Nikolic WV, Bai Y, Obregon D, Hou H, Mori T, Zeng J, et al. Transcutaneous beta-amyloid immunization reduces cerebral beta-amyloid deposits without T cell infiltration and microhemorrhage. Proc Natl Acad Sci U S A 2007;104:2507–12.

Expert Opinion

Tight junction modulator and drug delivery

Koji Matsuhisa, Masuo Kondoh†, Azusa Takahashi & Kiyohito Yagi
Osaka University, Graduate School of Pharmaceutical Sciences, Department of Bio-Functional Molecular Chemistry, Osaka, Japan

Recent progress in pharmaceutical technology based on genomic and proteomic research has provided many drug candidates, including not only chemicals but peptides, antibodies and nucleic acids. These candidates do not show pharmaceutical activity without their absorption into systemic flow and movement from the systemic flow into the target tissue. Epithelial and endothelial cell sheets play a pivotal role in the barrier between internal and external body and tissues. Tight junctions (TJs) between adjacent epithelial cells limit the movement of molecules through the intercellular space in epithelial and endothelial cell sheets. Thus, a promising strategy for drug delivery is the modulation of TJ components to allow molecules to pass through the TJ-based cellular barriers. In this review, we discuss recent progress in the development of TJ modulators and the possibility of absorption enhancers and drug-delivery systems based on TJ components.

Keywords: absorption enhancer, claudin, drug delivery, occludin, paracellular route, tight junction

Expert Opin. Drug Deliv. (2009) 6(5):509-515

1. Introduction

Drug candidates, including chemicals, peptides, proteins, nucleic acids and their derivatives, can be efficiently identified by a combination of high-throughput technology and genome-based drug discovery. However, two steps are required for the clinical application of these drug candidates: movement of the molecules into the body and tissue through epithelial and endothelial cell sheets. These cell sheets regulate the movement of solutes between tissues within the body as well as between the outside and inside of the body.

Routes for passing of drug through the epithelial and endothelial cell sheets are classified into transcellular and paracellular routes (**Figure 1**). In the transcellular route, drugs are delivered by simple diffusion into the cell membranes and active transport via a receptor or transporter on the cell membrane [1,2]. Various transporters involved in the influx and efflux of peptides, organic anions and cations have been identified, and transcellular delivery systems using the transporters have been widely investigated [2-6]. Transporter-mediated drug delivery is tissue-specific and has low toxicity; however, the drugs must be modified for interaction with the transporter without loss of pharmaceutical activity. Thus, the transcellular route is not suitable for high-throughput production of drug candidates. The other route for drug delivery is the paracellular route. Tight junctions (TJs) seal the paracellular route and prevent the free movement of molecules in the paracellular space; therefore, a strategy for the paracellular delivery of drugs is the opening of TJs [7,8]. Compared with the transcellular route, the paracellular route has the advantages that drug modification is not needed and that one method can be applied for various drugs. Drug delivery systems through the paracellular route have been investigated as absorption enhancers since the 1980s. However, only sodium caprate is currently used as an absorption enhancer in pharmaceutical therapy.

informa
healthcare

10.1517/17425240902902315 © 2009 Informa UK Ltd ISSN 1742-5247

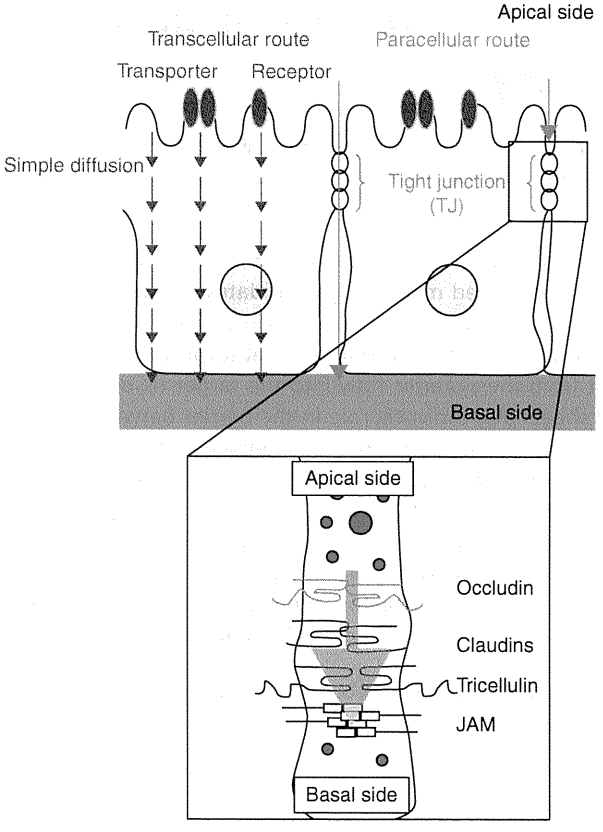

Figure 1. Schematic illustration of transport routes in epithelia.

It had been unclear how TJs regulated movement of solutes and what TJs were. In 1993, Furuse and colleagues determined that occludin, a protein with four transmembrane domains, is a component of TJs and that TJs consist of protein [9]. In 1998, Furuse and co-workers also identified another TJ protein, claudin-1 and -2 [10]. Claudins, a multigene family of at least 24 members, are key molecules of the TJ barrier [11]. Schematic biochemical machinery of TJs is shown in Figure 1, and modulation of the TJ components to allow drugs to pass through the paracellular route has been investigated as a novel strategy for drug delivery since the first report of TJ component-based drug delivery using an occludin peptide corresponding to part of the extracellular loop [12].

In this review, we examine recent topics in TJ-based drug delivery systems that use both approaches – TJ component/TJ modulator and TJ barrier – and discuss the future direction of such systems.

2. TJ components and TJ modulators

In the first section, we reviewed recent progress in TJ modulators over the past 2 years with respect to TJ components and modulators of TJ barrier.

2.1 Claudin

Claudin is a four-transmembrane TJ protein with a molecular mass of around 23 kDa, and comprises a family of at least 24 members [10]. Expression of each claudin member varies among cell types and tissues [13,14]. Claudins are thought to polymerize and form TJ strands in a homomeric and heteromeric manner, and the combination and mixing ratios of different claudin species determine the barrier properties of TJs, depending on the tissues [11]. For instance, deletion of claudin-1 causes dysfunction of the epidermal barrier [15], and deletion of claudin-5 causes dysfunction of the blood–brain barrier [16]. These findings indicate that a specific claudin modulator would be useful for tissue-specific drug delivery through the paracellular route. The C-terminal receptor binding region of *Clostridium perfringens* enterotoxin (C-CPE) is the only known modulator of claudin-4 [17]. Cells treated with C-CPE have decreased intracellular levels of claudin-4 as well as disrupted TJ barriers in epithelial cell sheets [17]. We previously found that the jejunal absorption-enhancing effect of C-CPE was 400-fold more potent than that of sodium caprate, the only clinically used absorption enhancer [18]. The development of other claudin modulators by using C-CPE as a prototype is a promising strategy. Deletion assays and site-directed mutagenesis assays indicate that the C-terminal 16 amino acids of C-CPE are involved in its modulation of claudin-4 and that Tyr residues at positions 306, 310 and 312 are critical for C-CPE activities [19,20]. Van Itallie and colleagues revealed that the structure of C-CPE is a nine-strand β sandwich and that the C-terminal 16–amino acid fragment is located in the loop region between the β8 and β9 strands, indicating that the claudin-4 binding site is on a large surface loop between strands β8 and β9 or on a domain containing these strands [21]. These findings indicate that peptides containing the loop structure formed by the β8 and β9 strands are likely to be novel claudin modulators. Considering the antigenicity of the claudin-4 modulator, smaller peptides are useful. Recently, the 12-mer peptide binders of claudin-4 were successfully identified using a random 12-mer peptide phage-display library [22]. The common claudin-binding motif <XX(Y/W)$(X)_{3\ or\ 4}$Y(Y/X)(L/I)XX> was also detected. The 12-mer peptide was bound to claudin with nanomolar affinity, but it did not modulate the claudin barrier. A 27-mer amino acid peptide corresponding to the extracellular loop region of claudin-1 modulated epithelial barrier through its interaction with claudin-3 [23]. Distinct species of claudins can interact within and between tight junctions [24]. Thus, a short peptide corresponding to the extracellular loop region of the heterotypically interacting claudin is also a candidate of claudin modulator.

2.2 Occludin

Occludin, a 65-kDa protein containing four transmembrane domains, was the first TJ-associated integral protein to be identified [9]. The initial strategy for TJ component-based